



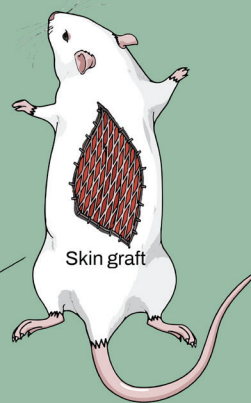
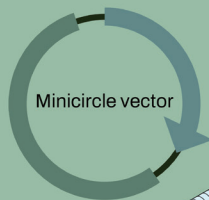
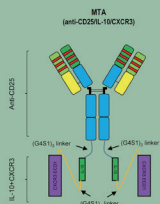
Therapeutic effect of multiple functional minicircle vector encoding anti-CD25/IL-10/CXCR3 in allograft rejection model

Sun Woo Lim^{1,2,*}, Yoo Jin Shin^{1,2,*}, Sheng Cui^{1,2}, Eun Jeong Ko^{1,2,3}, Seok Ho Yoo⁴, Byung Ha Chung^{1,2,3}, and Chul Woo Yang^{1,2,3}

¹Transplant Research Center, College of Medicine, The Catholic University of Korea, Seoul; ²Convergent Research Consortium for Immunologic Disease, ³Division of Nephrology, Department of Internal Medicine, Seoul St. Mary's Hospital, College of Medicine, The Catholic University of Korea, Seoul; ⁴Y-Biologics, Daejeon, Korea

Therapeutic effect of multiple functional minicircle vector encoding anti-CD25/IL-10/CXCR3 in allograft rejection model

Anti-CD25/IL-10/CXCR3 protein drug



Improved immunologic regulation

Th1, Th2, and Th17 ↓
Regulatory T cell ↑



**Prolonged skin allograft survival
Reducing allograft rejection**

Conclusion

- Self-generated anti-CD25/IL-10/CXCR3 protein drug by minicircle technology is functionally active and relevant for reducing allograft rejection.
- The minicircle vector system may be useful for developing new biological drugs, avoiding manufacturing or practical problems.

Received : June 30, 2021
Revised : January 3, 2022
Accepted : January 4, 2022

Correspondence to Chul Woo Yang, M.D.

Division of Nephrology, Department of Internal Medicine, Seoul St. Mary's Hospital, College of Medicine, The Catholic University of Korea, 222 Banpo-daero, Seocho-gu, Seoul 06591, Korea
Tel: +82-2-2258-6851, Fax: +82-2-2258-6917, E-mail: yangch@catholic.ac.kr
https://orcid.org/0000-0001-9796-636X

*These authors contributed equally to this work.

Background/Aims: We previously proposed minicircle vector technology as the potential platform for the development and production of new biologics. In this study, we have designed a novel target molecule for the treatment of allograft rejection and evaluated its feasibility as the therapeutic agent in this disease using the minicircle vector system.

Methods: We engineered vectors to carry cassette sequences for anti-CD25, interleukin-10 (IL-10), and C-X-C motif chemokine receptor 3 (CXCR3) fusion protein, and then isolated minicircle vectors from the parent vectors. We verified the substantial production of anti-CD25/IL-10/CXCR3 fusion protein from minicircles and their duration in HEK293T cells and mice models. We also evaluated whether minicircle-derived anti-CD25/IL-10/CXCR3 has therapeutic effects in a skin allograft in mice model.

Results: We confirmed the production of anti-CD25/IL-10/CXCR3 from minicircle by its significant availability in cells transfected with the minicircle and in its conditioned media. After a single injection of minicircle by hydrodynamic injection via mouse tail vein, luminescence or red fluorescence was maintained until 40 days in the liver tissue, suggesting the production of anti-CD25/IL-10/CXCR3 protein from minicircles via protein synthesis machinery in the liver. Mice treated with the minicircle encoding anti-CD25/IL-10/CXCR3 showed prolonged skin allograft survival times accompanied by improved immunologic regulation e.g., reduction of the lymphocyte population of Th1, Th2, and Th17 and an induction of regulatory T cells.

Conclusions: These findings implied that self-generated anti-CD25/IL-10/CXCR3 protein drug by minicircle technology is functionally active and relevant for reducing allograft rejection. The minicircle vector system may be useful for developing new biological drugs, avoiding manufacturing or practical problems.

Keywords: Biological products; Transplantation; Minicircle DNA; Graft rejection; Immune tolerance

INTRODUCTION

Kidney transplantation (KT) is still the best treatment choice for end-stage renal disease. However, acute rejection remains to be a common complication in KT and is associated with reduced graft survival [1]. Since 1995, the rates of acute rejection have fallen dramatically [2], partly owing to the increased use of induction therapy using biologics, such as rituximab, basiliximab, bortezomib, and so on, and the development of precise and selective induction agents. Biologics are now widely used in various transplant centers [2,3], either routinely or for high-risk individuals. The wide use of biologics for KT has made way for a new era in novel drug development. Because signal blockade can be achieved more easily using biologics, such as antibodies and soluble receptors, than using chemical drugs, target selection is an effective strategy for the development of novel drugs. Numerous proteins with major roles in KT can be considered as target biologics [4]. Although biologic agents are the key to successful allograft function, their development at a small scale is nearly impossible owing to the high cost of their purification and functional characterization [4-6]. Thus, a new approach to the development and evaluation of novel biologics is required.

Biologics, defined as synthetic drugs that are composed of peptide components, have made significant contributions to the treatment of transplant rejection, cancer, and immune disorders that were previously complex to treat [4,7]. Biologics have become extensively used in clinical practice, and it seems obvious that they have opened up a new period in the development of novel drugs. Because signal inhibitors can be more easily achieved using biologics, such as antibodies and soluble receptors, than with chemical drugs, target choice enables the generation of new drugs. Numerous proteins, containing cytokines and chemokines that play major roles in the pathogenesis of various diseases, can be considered as targets for biologics [7,8]. However, it is almost impossible to generate new biologics on a small scale because of their purification and functional characterization are costly. Thus, a new approach to the generation and evaluation of novel biologics, which has a relatively low cost and can be achieved over a short time frame, is needed.

We have previously proposed the minicircle (MC) vector system as an alternative approach for the development and production of biologics. MCs are protein-expressing vectors, in which the bacterial backbone has been removed [9]. As bacterial backbone components are not necessary for gene expression and may induce an immune response in mam-

malian cells, MCs are considered ideal plasmids for transgene expression *in vitro* and *in vivo* [10,11]. MCs are smaller than conventional plasmids, increasing the probability of cell delivery. Moreover, MCs escape gene silencing and show sustained expression because of the unique methylation patterns in these vectors [12]. Owing to these advantages of MCs, we, along with others have used them as tools for transgenic expression in animals. Some studies have delivered MCs encoding natural proteins, including hypoxia-inducible factor-1 α , α -1-iduronidase, interferon- γ (IFN γ), interleukin-23 (IL-23), and cytotoxic T lymphocyte-associated antigen-4-Ig (CTLA4Ig) into an animal model to examine the efficiency of MCs [13-17]. We also have delivered MCs encoding tocilizumab (anti-soluble interleukin-6 receptor [sIL-6R] antibody) and/or etanercept (tumor necrosis factor receptor 2 [TNFR2]-Fc fusion protein) and evaluated its efficacy in allograft rejection models [18]. Using this method, it is conceptually feasible to induce the production of a protein drug by the host using *in vivo* transfection of vectors carrying the full sequence of the protein drug.

Based on this protein drug delivery platform, we tried to evaluate the therapeutic effect of new synthetic protein on the allograft rejection. Especially in this study, we designed the MCs encoding multiple target-directed agents (MTAs) for the treatment of allograft rejection. We generated MC vectors containing the nucleotide sequences of basiliximab (anti-CD25 antibody), IL-10, and C-X-C motif chemokine receptor 3 (CXCR3), based on the backbone of an MC structure. Treatments using anti-CD25 antibody agents had significantly lower acute rejection rates than induction therapy [19,20]. However, because it also has the same effect on T regulatory (Treg) cells, IL-10 cells conjugated with anti-CD25 antibody compensated for the downregulation of Treg cells [21-23], because Treg cells are critical regulators of immune tolerance in transplantation [24,25]. In addition, CXCR3 is a dominant factor directing T cells into the allograft confirmed by highly up-regulated T cells [26]. Based on these findings, we designed the MTA structure by the fusion of the anti-CD25 antibody and IL-10 and CXCR3. In this study, the intravenous injection of the MC encoding MTA, which contained basiliximab, IL-10, and CXCR3 fusion, induced the *in vivo* production of new synthetic protein drugs. We found that self-produced MTA by the host were functionally active and reduced allograft rejection in a mouse model by using this platform technology for therapeutic protein.

METHODS

Production of minicircles

The MC vectors MC-mock and MC-MTA (anti-CD25/IL-10/CXCR3) were produced as described previously [27]. It is noteworthy that MTA is a combination of anti-CD25 heavy chain (HC)-IL-10-CXCR3 and anti-CD25 light chain (LC), and anti-CD25 is a combination of MC-anti-CD25HC and LC. To construct the MCs, each sequence (Supplementary Tables 1 and 2) was subcloned into the mock plasmid pMC.EF1-MCS-T2A-RFP (or Luciferase [LUC])-SV40 PolyA, which was purchased from System Biosciences (Mountain View, CA, USA). The plasmid contained NheI and BamHI restriction sites, and the cloning outcome was confirmed by double digestion at the two sites. The MCs were produced based on the method previously described by Kay et al. [28]. Briefly, *Escherichia coli* ZYCY10P3S2T cells were transformed with the protein drug-encoding parent plasmids (PPs). *E. coli* cells were grown overnight at 37°C in Terrific Broth containing 50 μ g/mL of kanamycin and then the Luria-Bertani broth containing 0.02% L-(+)-arabinose was added to the *E. coli* cultures. The mixture was incubated at 30°C for 5 hours, and MC DNA was isolated using Nucleobond Xtra Purification Kits (Macherey-Nagel, Duren, Germany), according to the manufacturer's instructions.

Cell culture and MC transfection

HEK293T cells were cultured in Dulbecco's modified Eagle's medium (DMEM; Gibco, Gaithersburg, MD, USA), supplemented with 7.5% fetal bovine serum (Gibco), 100-U/mL penicillin, and 100- μ g/mL streptomycin. HEK293T cells were transfected with the protein drug-encoding MC vectors using the lipofectamine 2000 reagent (Invitrogen, Carlsbad, CA, USA), according to the manufacturer's instructions. Briefly, MC-anti-CD25HC-IL-10-CXCR3 and MC-anti-CD25LC were co-transfected into cells to produce MC-MTA. MC-mock was transfected alone as the control groups. Cells were transfected with lipofectamine alone in the negative control group. The expression of red fluorescence protein (RFP) in the cells was assessed using fluorescence microscopy at 48 hours post-transfection. The transfected cell culture medium was collected for enzyme-linked immunosorbent assay (ELISA) to quantify the levels of the protein drug. The media were replaced 24 hours before collection, and conditioned media were collected at 5 days after transfection.

Ethics statement

All procedures were performed in strict accordance with the recommendations of the ethical guidelines for animal studies. All experimental animal care protocols were approved by the Animal Care and Use Committee of the Catholic University of Korea (CUMC-2018-0130). Animals were sacrificed under xylazine/rompun anesthesia, and every effort was made to minimize animal suffering.

In vivo gene delivery

MCs were delivered 1 day before skin grafting using the hydrodynamic tail-vein injection method [29]. Briefly, 40 µg of MC-anti-CD25HC-IL-10-CXCR3 and 40 µg of MC-anti-CD25LC were injected together into the MTA group to induce MC-anti-CD25-IL-10-CXCR3 production *in vivo*. Additionally, 40 µg of MC-IL10-anti-CD25HC and 40 µg of MC-anti-CD25LC were injected together into the dual-target-directed agent encoding anti-CD25/IL-10 (dual target-directed agent [DTA]) group to induce anti-CD25/IL10 production *in vivo*. Next, 80 µg of MC-mock was injected into the control MC-mock group. MCs were injected in a volume equivalent to approximately 10% of the body weight of the mice. To increase hydrodynamic pressure, 27-gauge needles were used, and the injection was completed within 5 to 7 seconds. The blood was collected from the mice injected with the indicated MCs for ELISA to quantify protein drug levels. Animals were allowed to live from 0.5 to 40 days after injection. At each time point, injected mice were used for *in vivo* imaging, and the blood and liver tissues were then collected for ELISA and fluorescence microscopy.

In vivo imaging analysis for MC detection

To prevent the detection of autofluorescence signals from the digestive system, mice were made to fast for 12 hours before *in vivo* imaging analysis. Hair removal was also performed to prevent the detection of autofluorescence signals from hair. Multispectral images of luminescence were acquired using the Optical *in vivo* Imaging System-IVIS Lumina XRMS (PerkinElmer, Waltham, MA, USA). Regions of interest were analyzed using the Perkin Elmer imaging software.

ELISA

To analyze the level of anti-CD25, IL-10, and CXCR3 protein expression in transfected cells or injected mice, the culture

media from the transfected HEK293T cells or plasma collected from mice injected with MCs were analyzed using ELISA. The levels of IL-10 or CXCR3 were quantified using sandwich ELISA. Briefly, a 96-well microtiter plate was coated with each commercial anti-mouse IL-10 (MAB417-100, R&D Systems, Minneapolis, MN, USA; at a concentration of 1 mg/mL) or anti-mouse CXCR3 (NBP2-41250, Novus Biologicals, Centennial, CO, USA; at a concentration of 1 mg/mL) in coating buffer and was incubated overnight at 4°C. The plate was incubated with blocking solution for 1 hour, followed by incubation overnight at 4°C with 100 µL of serially diluted recombinant murine IL-10 (210-10, PeproTech, Rocky Hill, NJ, USA; used as a standard) or recombinant mouse CXCR3 (MBS1172599, MyBioSource, San Diego, CA, USA; used as a standard), and the samples of conditioned media or plasma. Anti-mouse IL-10 biotinylated antibodies (BAF417, R&D Systems) or anti-murine CXCR3 biotinylated antibodies (MBS541349, MyBioSource) were applied to the wells and incubated for 2 hours. After incubation with anti-streptavidin-horseradish peroxidase (HRP) (DY998, R&D Systems) for 20 minutes, the TMB substrate solution (DY999, R&D Systems) was applied to each plate for 20 minutes.

Indirect ELISA was performed to determine the levels of anti-CD25. Briefly, a 96-well microtiter plate was coated with recombinant human sCD25 (21-8702-U100, TONBO Biosciences, San Diego, CA, USA) at a concentration of 1 mg/mL in coating buffer and was incubated overnight at 4°C. The plate was incubated with blocking solution for 1 hour, followed by incubation with 100 µL of serially diluted basiliximab (Simulect, Novartis Pharma AG, Basel, Switzerland; used as a standard) and the samples of conditioned media or plasma overnight at 4°C. After incubation with anti-human immunoglobulin G (IgG)-HRP (AP112P, Merck Millipore, Billerica, MA, USA) for 2 hours, the TMB substrate solution (DY999, R&D Systems) was applied for 20 minutes. Absorbance was then measured at 405 and 570 nm.

To identify the fusion complex of MTA, a 96-well microtiter plate was coated with recombinant human sCD25 (21-8702-U100, TONBO Biosciences) at a concentration of 1 mg/mL in coating buffer and was incubated overnight at 4°C. The plate was incubated with blocking solution for 1 hour. and then anti-human IL-10 biotinylated antibodies (BAF217, R&D Systems) or anti-murine CXCR3 biotinylated antibodies (MBS541349, MyBioSource) were applied to each plate for 2 hours. After incubation with anti-strepta-

vidin-HRP (DY998, R&D Systems) for 20 minutes, the TMB substrate solution (DY999, R&D Systems) was applied for 20 minutes.

Transwell migration assay

The upper chambers have membranes with 8- μ m pore size (Corning Incorporated, Kennebunk ME, USA). Before performing migration assay, HEK293T cells were seeded in the upper chambers and transfected MC-MTA. Chemokine (C-X-C motif) ligand (CXCL) 9, 10, and 11 (#250-18, 250-16, 250-29, PeproTech, Cranbury, NJ, USA) were added in the lower chamber after 48 hours. After 24 hours of incubation, migrated cells on the underside of the trans-well membrane were fixed with methanol and stained with 1% toluidine blue. The migrated cells were counted and averaged from six random fields.

Skin allograft rejection in mice

For the experimental skin graft model, the protocol described by McFarland and Rosenberg [30] was employed. Briefly, C57BL/6 mice were used as donors for skin transplantation. Skin from the donor tail (1.0 cm²) was placed on the back of BALB/c recipients. The recipient mice were transplanted with MC-mock injection, MC-DTA, or MC-MTA injection with or without daily administration of tacrolimus (Tac, Astellas Pharma, Ibaraki, Japan; 2 mg/kg/day diluted in distilled water) by gavage for 17 days, starting 3 days prior to transplantation. Graft rejection was defined as the complete destruction or desiccation of the grafted skin on inspection. Graft survival curves were constructed using the Kaplan–Meier method and graft survival was compared between two groups using the log-rank test. The skin grafts were removed at the indicated time points and rinsed in cold saline, immersed in 4% paraformaldehyde for 2 hours at 4°C, and embedded in paraffin for histopathologic examination. Tissue sections (5 to 7 μ m) were stained with hematoxylin and eosin (H&E) for the assessment of cell infiltration.

EXPERIMENTAL DESIGN

In the MC-mock group (n = 5), mice were injected with 80 μ g of MC-mock intravenously 1 day before skin transplantation. In the MC-DTA encoding anti-CD25/IL-10 (n = 5), mice were injected with 40 μ g of MC-anti-CD25HC and 40 μ g of MC-anti-CD25LC intravenously 1 day before skin transplan-

tation. In the MC-MTA group (n = 5), mice were injected with 40 μ g of MC-anti-CD25HC-IL-10-CXCR3 and 40 μ g of MC-anti-CD25LC intravenously 1 day before skin transplantation. In the Tac + MC-DTA or MC-MTA groups (n = 5 in each group), mice received 2 mg/kg Tac daily by oral gavage, starting 3 days before transplantation, for 17 days in the MC-DTA and MC-MTA groups.

Immunohistochemistry

Deparaffinized tissue sections were incubated in retrieval solution (pH 6.0), methanolic H₂O₂, and 0.5% Triton X-100 and were then washed in phosphate-buffered saline. Non-specific binding sites were blocked in 10% normal donkey serum (Jackson ImmunoResearch Laboratories, West Grove, PA, USA). Sections were incubated overnight at 4°C with the following antibodies: monoclonal rabbit anti-CD4 (1:100; ab183685, Abcam, Cambridge, UK) and monoclonal rat antibody against mouse IL-10 (1:50; BD559063, BD Biosciences, San Jose, CA, USA). Primary antibody binding was visualized using the following secondary antibodies: Cy3-conjugated goat anti-rabbit antibody (1:1,000; Jackson ImmunoResearch) and Alexa Fluor 488-conjugated goat anti-rat antibody (1:200; ThermoFisher, Waltham, MA, USA). Stained tissues were viewed using a fluorescence microscope (Axio imager M2, Carl Zeiss Co. Ltd., Oberkochen, Germany). Images were converted to the tagged image file format (TIFF), and contrast levels were adjusted using Adobe Photoshop v. 13 (Adobe System, San Jose, CA, USA). Immunolabeling profiles of skin grafts were evaluated by counting approximately 10 randomly selected areas (22,534.06 μ m² per field) in each stained tissue section at \times 100 magnification using an image analysis software (Celleste version 5.0.2, ThermoFisher).

Flow cytometry

The expression of cytokines and transcription factors was assessed using cell surface and intracellular staining. At day 5 after skin grafting, single-cell suspensions of the spleens of mice were prepared and stained with fluorescently labeled monoclonal antibodies. Splenocytes were stained with various combinations of fluorochrome-conjugated antibodies against CD4 and CD25. Intracellular flow cytometry for cytokines (IFN γ , IL-4, and IL-17) and the transcription factor forkhead box P3 (Foxp3) was also performed using either Cytofix/Cytoperm (BD Biosciences, San Jose, CA, USA) or fixation/permeabilization buffer (eBioscience, San Jose, CA,

USA), according to the manufacturer's instructions. Appropriate isotype controls were always included. All samples were analyzed using a FACS LSRFortessa (BD Biosciences) and FlowJo software (FlowJo LLC, Ashland, OR, USA).

Statistical analysis

Data are expressed as mean ± standard deviation of at least three independent experiments. Comparisons among groups were performed using one-way analysis of variance with Bonferroni's *post hoc* test using GraphPad Prism version 7.03 for Windows (GraphPad Software, La Jolla, CA, USA). Statistical significance was set at a value of $p < 0.05$.

RESULTS

Construction and generation of MC encoding MTA

Because the blocking of CD25 and the production of IL-10 in T cells play important roles in preventing allograft rejection, we previously designed a DTA [31]. In this study, we designed the MTA as the CXCR3 sequence conjugated to the anti-CD25 antibody and IL-10 sequence by linkers (Supplementary Tables 1 and 2). To generate the fusion form, the nucleotide sequences of anti-CD25HC attached to the 3' end of the sequences encoding the IL-10 and CXCR3 sequence and the anti-CD25LC sequences were subcloned into the PP separately (PP-anti-CD25HC-IL-10-CXCR3 and PP-anti-CD25LC). We predicted that the transfection of both plasmids into cells would lead to the construction of the intact form of the anti-CD25/IL10/CXCR3 fusion protein (Fig. 1). Each insert was subcloned downstream of the EF1 promoter, and RFP or LUC sequences were placed under the control of the EF1 promoter (Fig. 2A).

The two plasmids were transfected into a single cell to generate an intact anti-CD25/IL-10/CXCR3 protein drug. After PPs were treated with L-arabinose, MCs were generated, downsized by phage ΦC31, and the bacterial backbone was degraded. The ΦC31 integrase combines the attB and attP sites of the PP vector, resulting in the production of two circular DNAs (the MC plasmid and bacterial backbone) (Fig. 2B). Purified MCs were used for subsequent experiments.

We confirmed that the expressible DNA sequences of each protein drug were subcloned into the PP by digestion with XbaI and BamHI (Fig. 2C). We detected a band corresponding to the size of the insert. We also confirmed that the

whole DNA sequences intended for subcloning were contained in the PP by DNA sequencing. Supplementary Table 2 provides the peptide sequences of the protein drugs. We also confirmed that the PPs encoding protein drugs were properly converted to MCs after treatment with L-arabinose (Fig. 2D). After digestion with NheI and BamHI, the DNA fragments of interest were detected in the MCs (Fig. 2E).

Protein drug production *in vitro* using MC encoding MTA

To investigate whether MCs are expressed *in vitro*, we examined RFP expression after the transfection of PPs and MCs into HEK293T cells. Higher RFP expression was observed by fluorescence microscopy in the MC group than in the PP group (Fig. 3A). The culture media of transfected cells were collected, and the levels of the anti-CD25, IL-10, and CXCR3 proteins were assessed by ELISA using CD25, anti-IL10, and anti-CXCR3-coated plates, respectively. MCs carrying the DNA sequences of the protein drug yielded efficient expres-

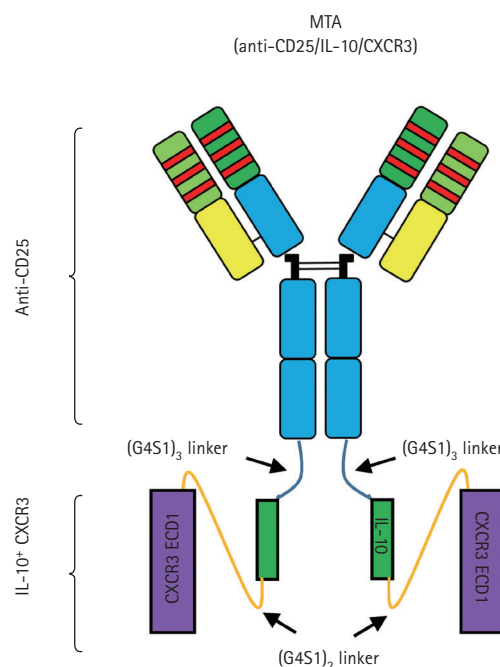


Figure 1. Diagram of the novel multiple target-directed agent (MTA), which was constructed as an anti-CD25 antibody conjugated to interleukin-10 (IL-10) and C-X-C motif chemokine receptor 3 (CXCR3) in turn at the end of the Fab region. MTA structure designed by the fusion of the anti-CD25 antibody and the dimer form of IL-10 via short flexible linkers, called (G4S1)₃ linker. CXCR3 was connected with IL-10 using the (G4S1)₂ linker. (G4S1)₃, (GGGS)₃; (G4S1)₂, (GGGS)₂; mIL-10, mouse interleukin-10; mCXCR3, mouse C-X-C motif chemokine receptor 3; ECD1, extracellular domain 1.

sion of each drug in the culture media at day 3 (Fig. 3B-3D).

Protein drug production *in vivo* using MC encoding MTA

To investigate the persistence of MC expression *in vivo*, we

examined luminescence expression after the hydrodynamic tail vein injection of MC-MTA into mice using *in vivo* imaging, mainly in the abdomen. Supplementary Figs. 1-3 showed no significant differences in body weight and basic functions between the MC-mock and MC-MTA groups

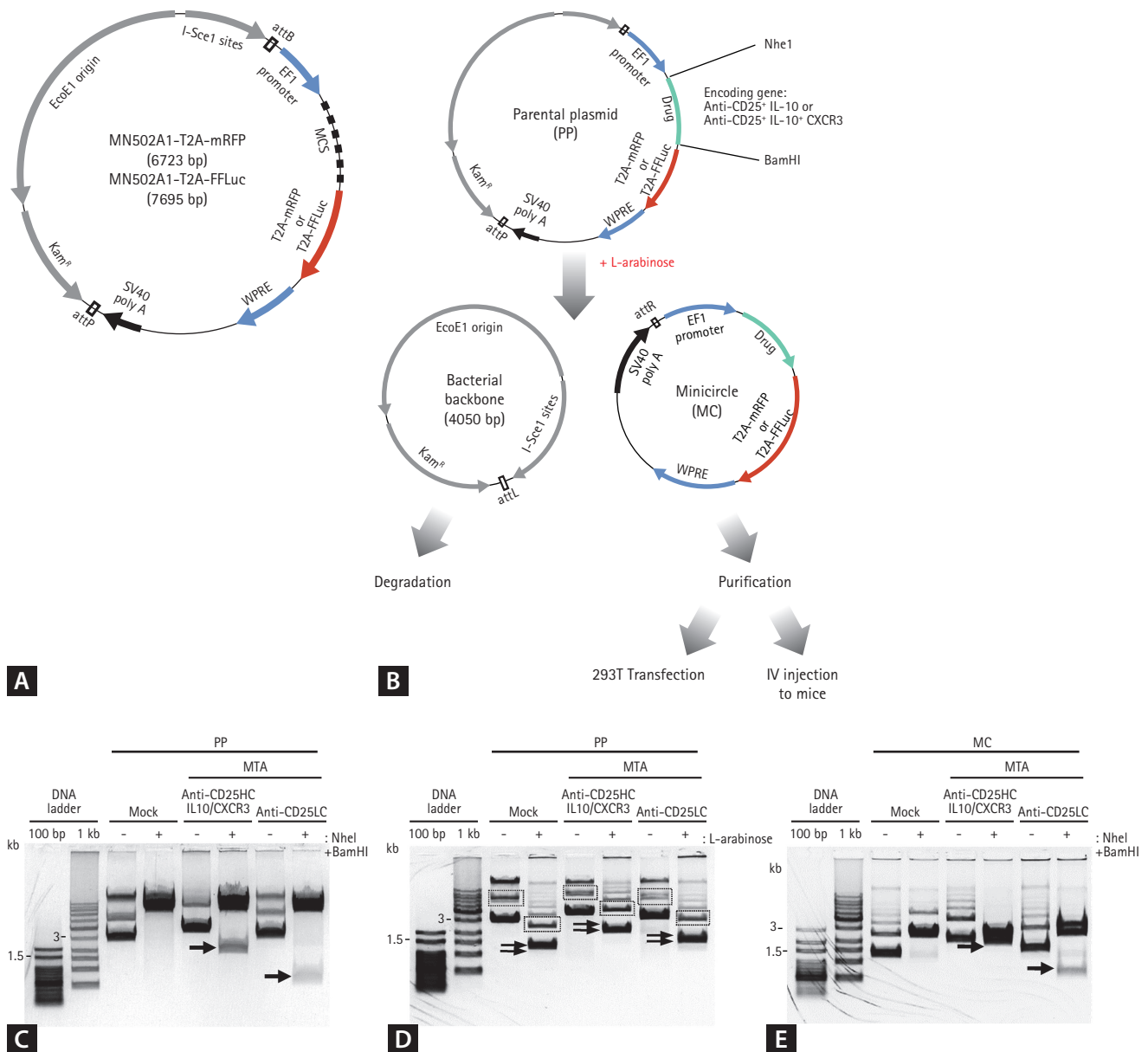


Figure 2. Generation of the minicircle (MC) encoding multiple target-directed agent (MTA). (A) Vector map of the parent plasmid (PP) pMC.EF1-MCS-T2A-RFP (or LUC)-SV40PolyA (PP-mock). (B) Diagram of the procedure for MC production. After incubation with 0.02% L-arabinose, site-specific recombination between the attB and attP sites was performed by bacteriophage ΦC31 integrase to generate MCs devoid of the bacterial-backbone DNA, which was degraded by I-SceI endonucleases and bacterial exonucleases. MCs were purified and used for further experiments. (C) Gel electrophoresis data for PPs digested with NheI and BamHI. Arrow indicates bands of the expected size for the insert. (D) Gel electrophoresis data for PPs before and after arabinose induction (open rectangles). Dotted rectangles indicate bands of the expected size for MCs derived from PPs. Double arrows indicate supercoiled plasmid DNA, which is more efficient in cellular transfection compared to the circular form (dotted rectangles). (E) Gel electrophoresis data of MCs digested with NheI and BamHI. Arrow indicates bands of the expected size for the insert. IV, intravenous.

(Supplementary Methods).

RFP expression was not observed in mice injected with saline. After MC-MTA injection, RFP levels increased from 1 to 13 days, and the enhanced expression was sustained until at least 40 days, which was the final time point examined (Fig. 4A and 4B). The hydrodynamic delivery method for MC injection temporarily upregulates the permeability of endothelial cells in the capillaries by increasing pressure [32,33]. The liver contains a large number of capillaries and is the most common site for gene delivery using this method [34-37]. Therefore, we evaluated RFP-positive cells in the liver tissues of mice injected with MCs. Numerous RFP-expressing cells were detected at 13 days and expression was

sustained for 40 days, consistent with the *in vivo* imaging results (Fig. 4C).

To assess the expression and secretion of anti-CD25/IL-10/CXCR3 derived from MC-MTA, plasma anti-CD25, IL-10, and CXCR3 levels were measured by ELISA on CD25, anti-IL-10, or anti-CXCR3-coated plate using plasma samples at 1, 7, and 30 days after injection with MC-MTA. MCs carrying the DNA sequences of the MC-MTA yielded the efficient expression of each drug at day 7. Anti-CD25/IL10/CXCR3 generation by the MC-MTA was retained until 30 days after MC-MTA treatment (Fig. 5A-5C). In addition, we compared the concentrations of anti-CD25, IL-10, and CXCR3 in each plasma sample at 3 days after the injection of PP-MTA

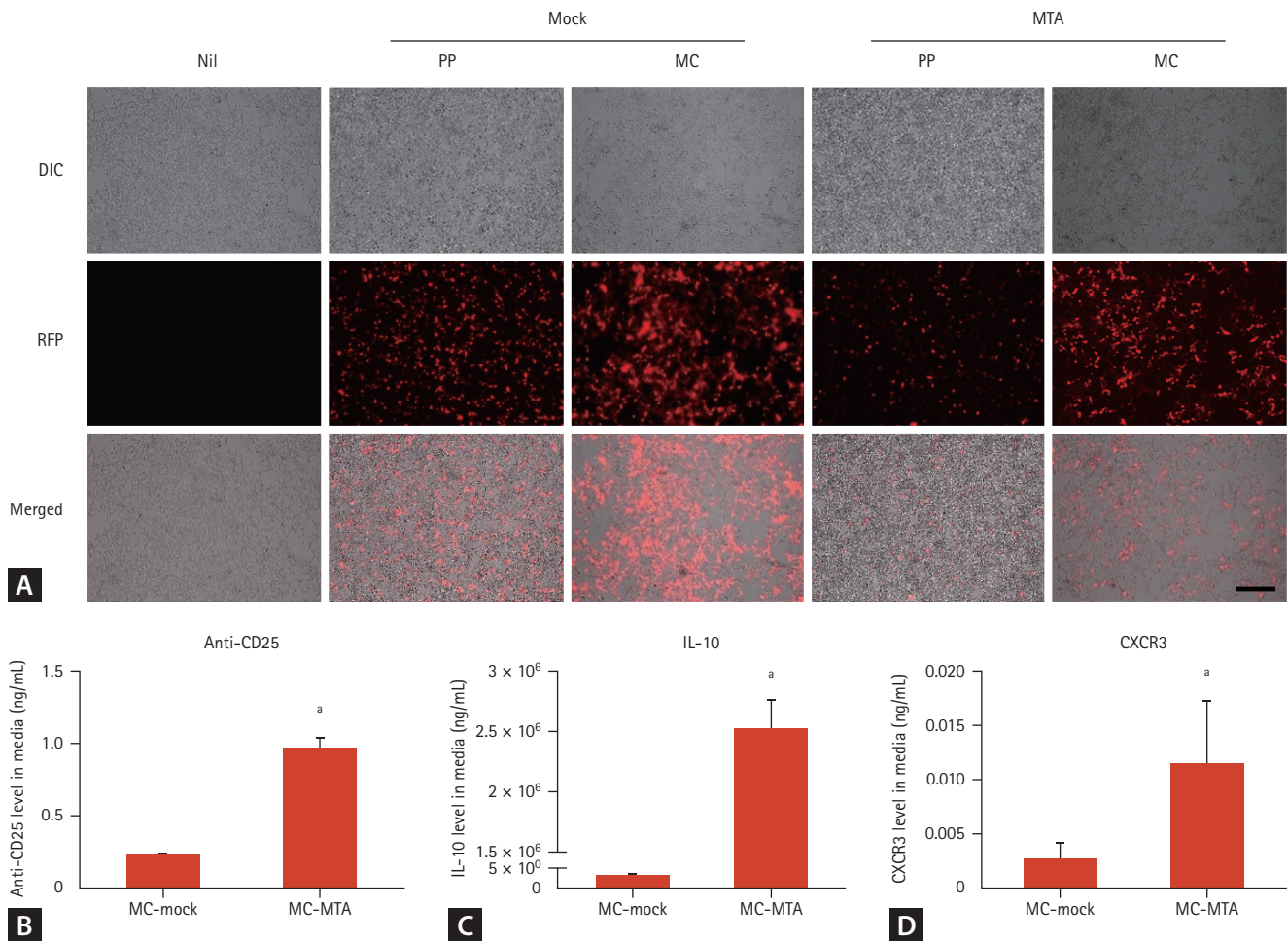


Figure 3. Detection of multiple target-directed agent (MTA) derived from minicircles (MCs) *in vitro*. (A) Fluorescence images of the expression of red fluorescence protein (RFP). HEK293T cells were transfected with the indicated DNA, and RFP expression was analyzed using fluorescence microscopy at 3 days post-transfection. HEK293T cells that were not transfected with DNA were used as a nil group. Scale bar = 50 μ m. (B, C, D) Concentrations of anti-CD25, interleukin-10 (IL-10), and C-X-C motif chemokine receptor 3 (CXCR3) in conditioned media of cells transfected with MC-mock or MC-MTA. Protein secretion from HEK293T cells was assessed using enzyme-linked immunosorbent assay (ELISA) at 3 days after transfection. Values are mean \pm standard error. All results are representative of at least three independent experiments. DIC, differential interference contrast; PP, parent plasmid. ^a*p* < 0.05 vs. MC-mock.

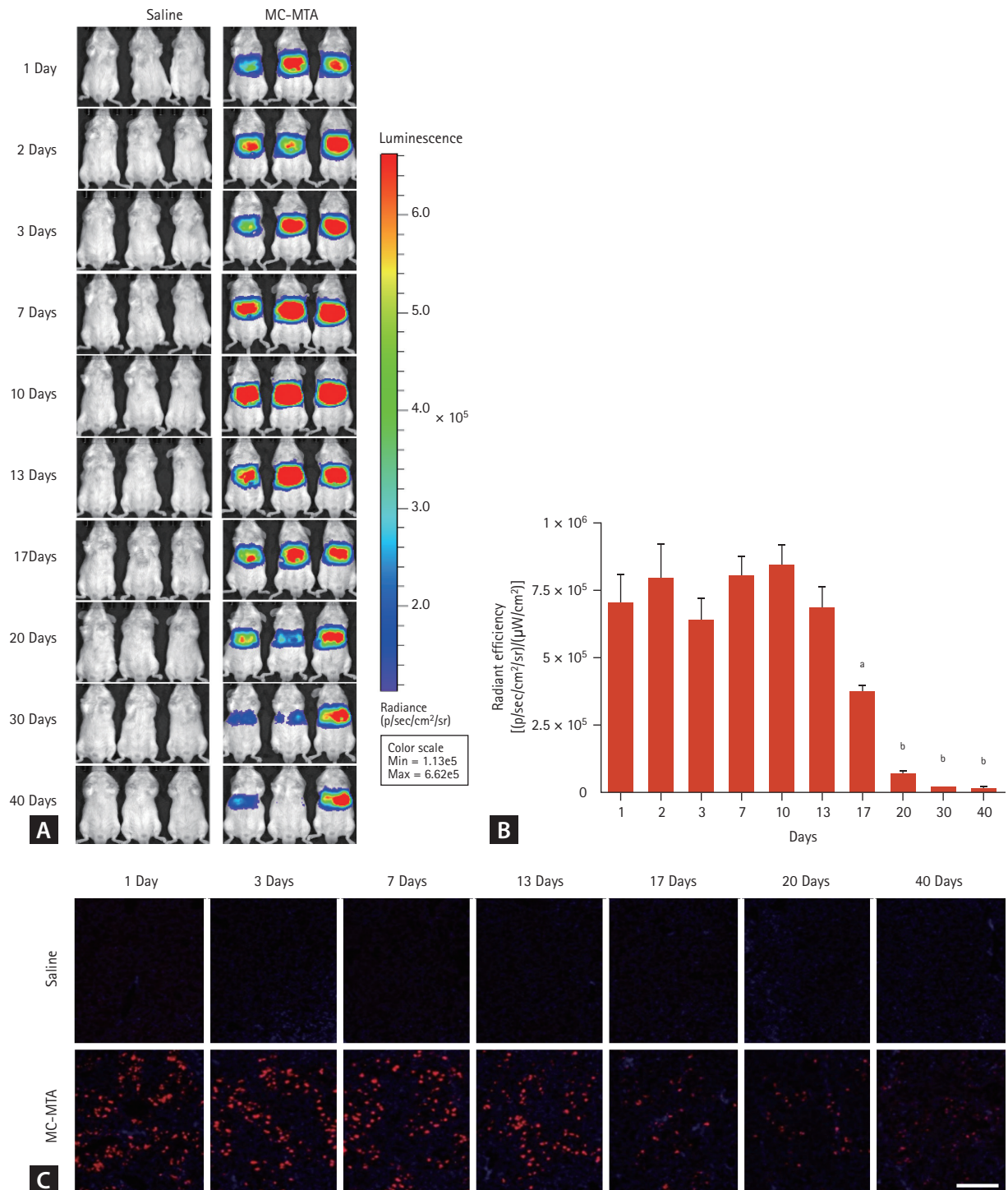


Figure 4. *In vivo* detection of multiple target-directed agent (MTA) derived from minicircles (MCs). Normal mice were treated with MC-MTA by tail vein injection using the hydrodynamic method, and negative control mice were injected with the same volume of normal saline. Mice were made to fast for 12 hours before *in vivo* imaging, followed by the assessment of luminescence (LUC) expression using the IVIS Lumina XRMS In Vivo Imaging System (PerkinElmer). (A) Representative images of mice each day after the injection of saline or MC-MTA obtained using the *in vivo* imaging system. Red fluorescence protein (RFP) was mainly detected in the upper portion of the body. (B) Radiant efficiency from *in vivo* imaging was calculated for the quantification of LUC after a single DNA injection at each time point. Note that the highest radiant efficiency of LUC was detected at 13 days, and was sustained until 40 days after injection. (C) RFP expression in mouse livers at each time point. A saline-treated group was used as a negative control. Scale bar = 200 μm. Values are mean ± standard error. All results are representative of at least three independent experiments. ^a*p* < 0.05 vs. day 17 group, ^b*p* < 0.01 vs. day 17 group.

or MC-MTA and found that the concentrations were higher in the MC-MTA group than in the PP-MTA group, as shown in Fig. 5D and 5F.

Cell migration function by MC encoding MTA *in vitro* and *in vivo*

We applied the transwell migration assay in the co-culture system to examine the consequences of increased migrating cells under ligands of CXCR3 e.g., CXCL9,10, and 11 (Fig. 6A). As shown in Fig. 6B and 6C, bottom chamber containing CXCLs showed promoted migration of MC-MTA transfected HEK293T cells into the bottom sides of the insert wells of the upper chamber compared with the normal media group (Fig. 6B and 6C). For *in vivo* migration of MC-MTA to the allograft, we delivered MC-MTA (tagging LUC or RFP) in the recipient of the skin allograft mouse model. We measured LUC around the transplanted skin allograft and found that LUC was detected in the allograft (Fig. 6D). RFP fluorescence was also stained with anti-RFP antibody

compared with the saline group (Fig. 6E).

Therapeutic effect of MC encoding MTA on skin allograft rejection

We used a highly immunogenic *in vivo* experimental skin allograft model to examine the function of the protein drug from the MC encoding anti-CD25/IL-10/CXCR3. One day before receiving a skin allograft, BALB/c recipients were injected with each MC using the hydrodynamic delivery method. Several animals were sacrificed for flow cytometry and H&E staining, and the remainder were visually inspected daily until complete graft rejection. Skin allografts in MC-mock-injected mice had a median survival time (MST) of 7.1 ± 0.3 days. The treatment of mice with MC-DTA resulted in the significant prolongation of skin allograft survival (10.4 ± 0.4 days, *p* < 0.05 vs. MC-mock). Interestingly, MC-MTA-injected mice showed longer MSTs than the other groups (11.4 ± 0.6 days, *p* < 0.05 vs. other groups) (Fig. 7A and 7B). We observed marked desmoplasia, hyalinization,

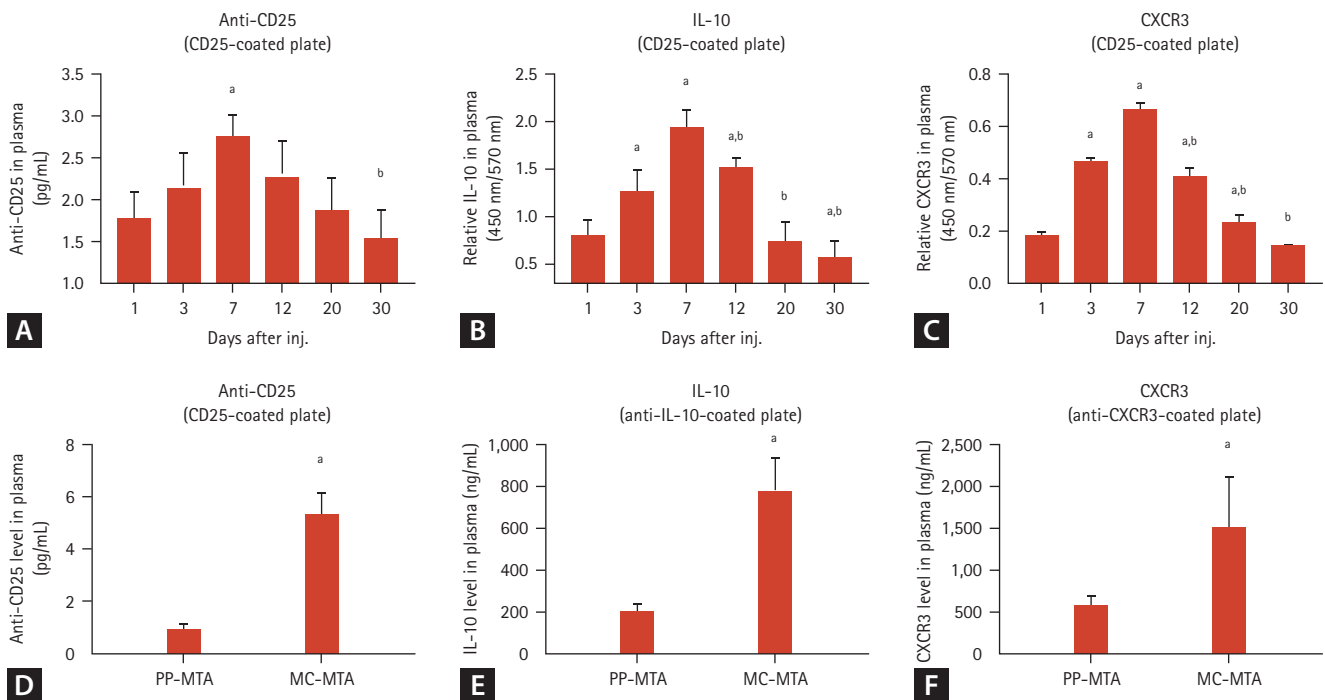


Figure 5. Detection of multiple target-directed agent (MTA) derived from minicircles (MCs) in normal mouse plasma using enzyme-linked immunosorbent assay (ELISA). (A, B, C) Concentration of anti-CD25, interleukin-10 (IL-10), and C-X-C motif chemokine receptor 3 (CXCR3) in the plasma of mice injected with MC-mock or MC-MTA. For the detection of the fusion protein form of MTA, recombinant CD25-coated plates were incubated with the plasma of mice injected with MC-MTA overnight. Detection was performed using an anti-human immunoglobulin G (IgG)-horseradish peroxidase (HRP), IL-10 biotinylated antibody, or CXCR3 biotinylated antibody and HRP-conjugated streptavidin antibody, respectively. (D, E, F) Concentrations of anti-CD25, IL10, and CXCR3 in the plasma of mice injected with parent plasmid (PP)-MTA or MC-MTA after 3 days. Values are mean ± standard error. All results are representative of at least three independent experiments. ^a*p* < 0.05 vs. MC-mock or PP-MTA, ^b*p* < 0.05 vs. 7 day group.

and inflammatory cell infiltration in the MC-mock-treated allogeneic control group, but the number of infiltrating cells was reduced in the MC-DTA group (4.5 ± 0.6 vs. 8.8 ± 1.4 , $p < 0.05$ vs. MC-mock group), with the greatest reduction in the MC-MTA-injected group (1.5 ± 0.6 , $p < 0.05$ vs. MC-DTA group) (Fig. 7C and 7D). Fig. 7E-7G shows immunoreactivity for CD4 or IL-10 and its quantitative analysis in skin allograft tissue section in each group. The number of CD4 positive cells was significantly lower in the MC-DTA group than in the MC-mock group ($168 \pm 18/\text{field}$ vs. $339 \pm 76/\text{field}$, $p < 0.05$ vs. MC-mock group). However, the MC-MTA group showed a further reduced number of CD4 positive cells compared with the MC-DTA group ($89 \pm 18/\text{field}$, $p < 0.05$ vs. MC-DTA group). On the contrary, the MC-MTA

group showed a higher number of restored IL-10 cells than the MC-mock and MC-DTA groups (235 ± 22 vs. $92 \pm 9/\text{field}$ in the MC-mock group and $159 \pm 25/\text{field}$ in the MC-DTA group, $p < 0.05$ vs. MC-mock and MC-DTA groups).

Next, we evaluated whether the prolonged skin allograft survival in the MC-MTA group is associated with the suppression of the pro-inflammatory T cell subset and induction of anti-inflammatory T cells (Treg cells). We performed flow cytometry to evaluate Th1, Th2, Th17, and Treg cells in splenocytes from the experimental animals. As shown in Fig. 8, the numbers of $\text{CD4}^+\text{IFN}\gamma^+$, $\text{CD4}^+\text{IL4}^+$, and $\text{CD4}^+\text{IL17}^+$ cells (i.e., Th1, Th2, and Th17 cells, respectively) were significantly lower in the MC-DTA and MC-MTA groups than in the MC-mock group. The number of positive cells was

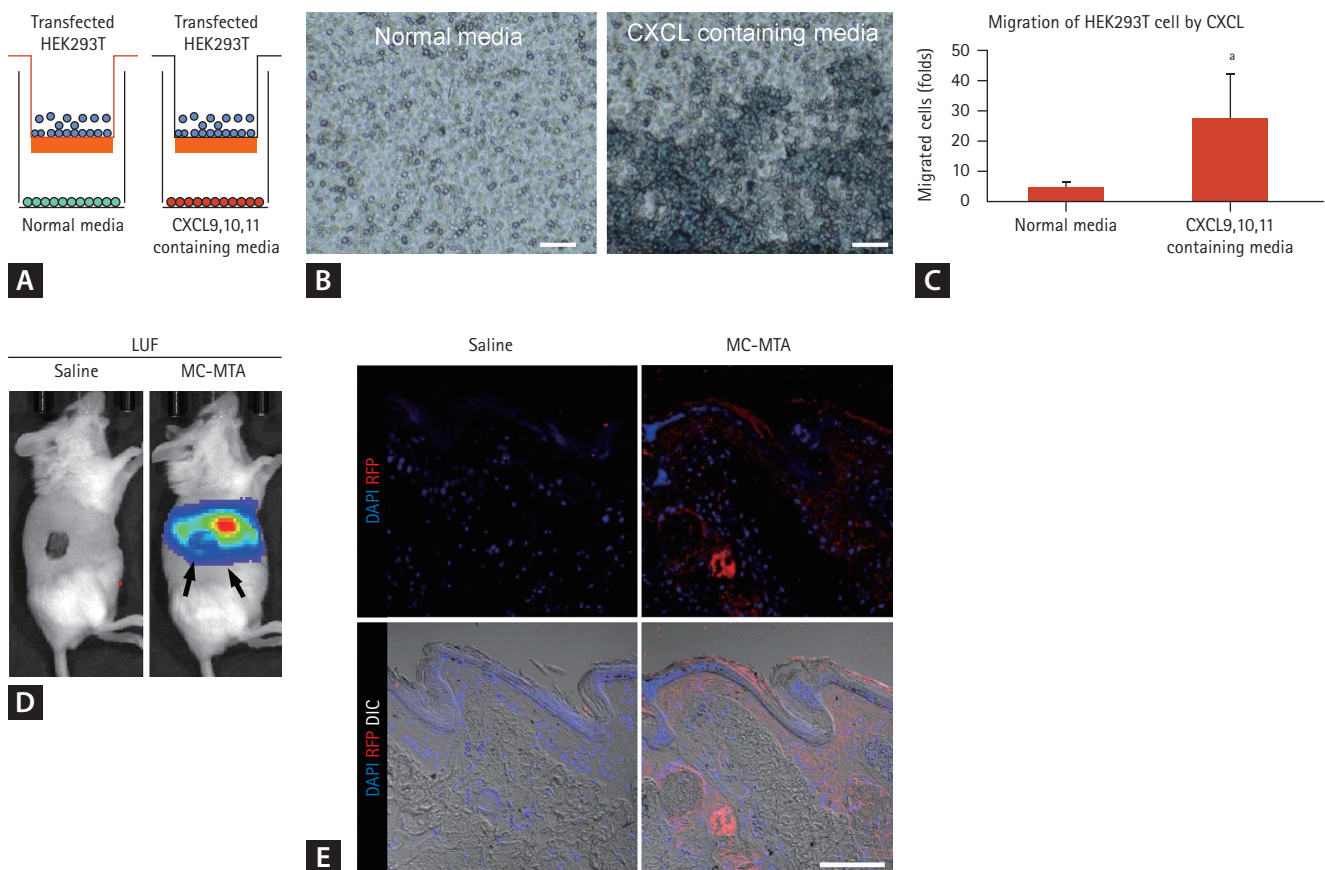


Figure 6. Migration function of minicircle (MC) encoding multiple target-directed agent (MTA). (A, B) Cartoon illustration of the migration assay for MC-MTA-transfected HEK-293T cell. The insert upper was plated with MC-MTA-transfected HEK-293T cells in serum free media, and chemokine (C-X-C motif) ligand (CXCL) 9, 10, and 11 were added to the lower well. The plates were incubated for 24 hours, and then cells that migrated into the lower well were fixed and stained to visualize the migrated cells. One representative experiment is shown. Scale bar = 50 μm . (C) Quantitation data for migrated HEK-293T cell by CXCLs. (D) Intravital image of saline or MC-MTA (tagging luminescence [LUC]) treated BALB/c recipients grafted with tail skin of C57BL/6 donor. Arrows denote the LUC activity in MC-MTA treated group. (E) A section of skin allograft with injected MC-MTA (tagging red fluorescence protein [RFP]) was stained with anti-RFP antibody (red fluorescence). LUF, luciferase; DAPI, 4',6-diamidino-2-phenylindole; DIC, differential interference contrast. Scale bar = 100 μm . ^a $p < 0.05$ vs. normal media.

the lowest in the MC-MTA group (Fig. 8A-8F). The population of CD4⁺ Treg cells (defined as CD4⁺CD25⁺Foxp3⁺ cells) increased significantly in the MC-DTA group and was the highest in the MC-MTA group than in the MC-mock group (Fig. 8G and 8H).

Combined effect of Tac and MC encoding MTA on skin allograft rejection

Although Tac is a first-line immunosuppressant in transplantation, it is associated with immunological complications [38-40]. Therefore, we compared allograft survival using

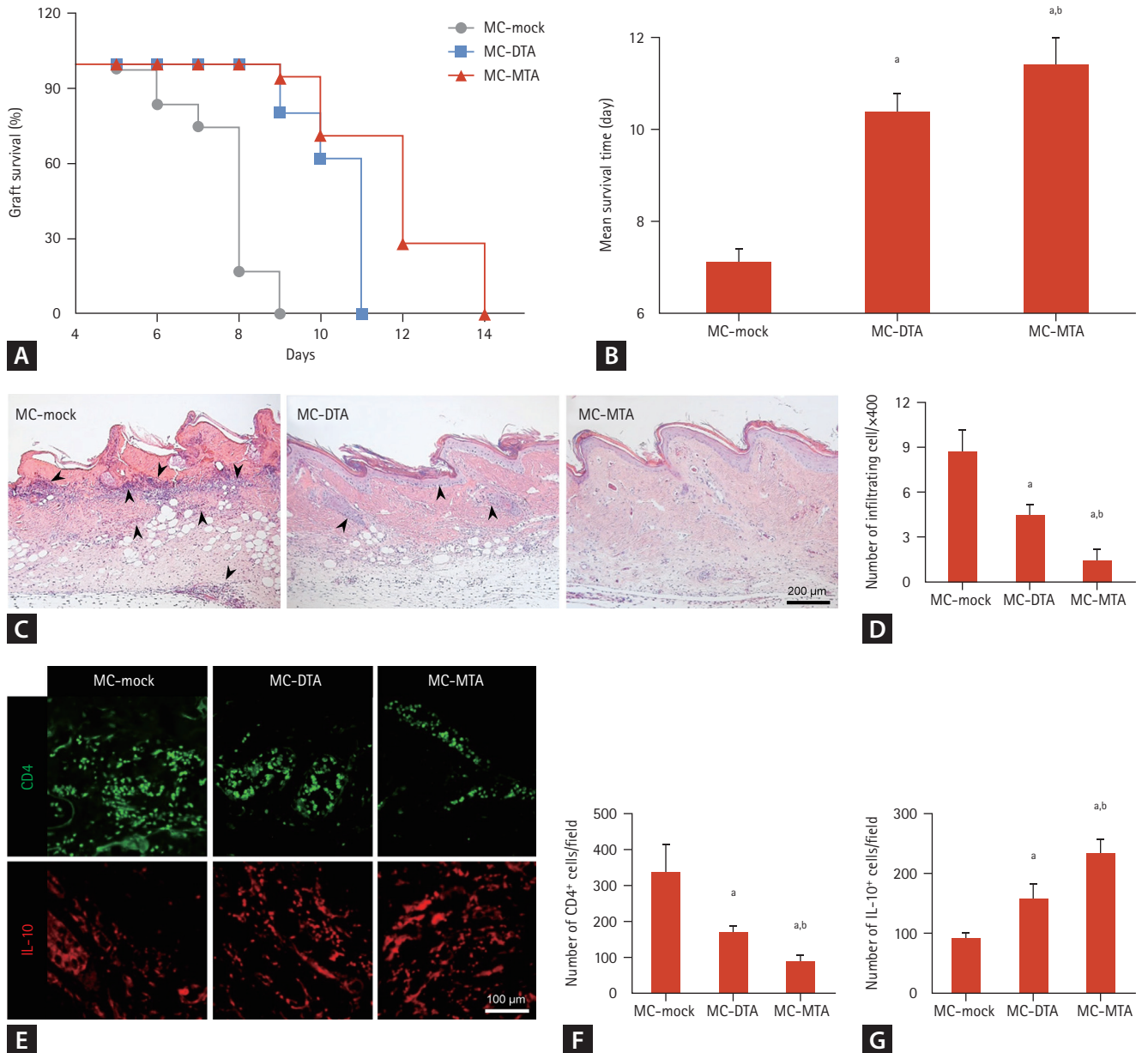


Figure 7. Skin allograft survival in mice treated with minicircle (MC) encoding multiple target-directed agent (MTA). (A, B) Survival curve and mean survival times of skin allografts in the MC-mock, MC-dual target-directed agent (DTA), or MC-MTA treated group. Administration of MC-MTA prolongs graft survival in BALB/c recipients compared with the MC-mock and MC-DTA-treated groups. (C, D) Representative images and quantitative graph of histological changes in skin allografts at day 5. Hematoxylin and eosin (H&E) staining was performed for each sample. MC-mock-treated group showed abundant immune cell infiltration in the derma of skin grafts (arrowheads) compared with the MC-DTA and MC-MTA groups. However, the MC-MTA group showed moderate infiltration compared with the MC-DTA group. (E, F, G) Representative immunofluorescence image and quantitative analysis for CD4 or interleukin-10 (IL-10) in the skin graft at day 5. (E) Scale bar = 200 μm in D and 100 μm. Values are mean ± standard error. ^a*p* < 0.05 vs. MC-mock, ^b*p* < 0.05 vs. the other group.

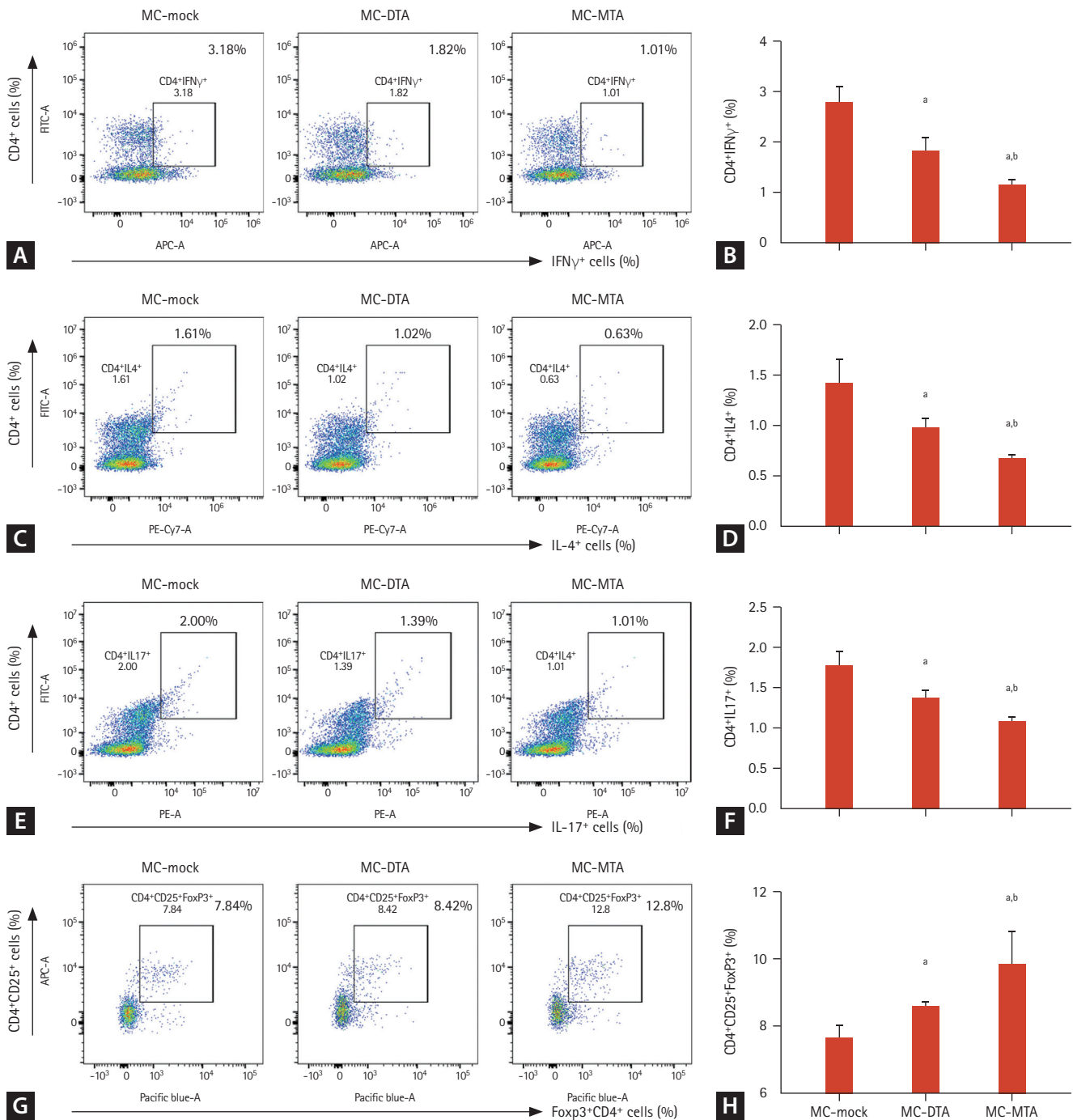


Figure 8. Effect of treatment with minicircle (MC) encoding multiple target-directed agent (MTA) on pro-inflammatory T cells and regulatory T cells. Lymphocytes were harvested from the spleens of mice at day 5 after the injection of MCs. Isolated lymphocytes were stimulated for 4 hours *ex vivo* with phorbol myristate acetate and ionomycin in the presence of GolgiStop before being fixed, stained, and permeabilized. After surface staining with anti-CD4, the number of lymphocytes expressing interferon- γ (IFN γ), interleukin-4 (IL-4), or IL-17 was measured by flow cytometry. For the detection of regulatory T cells, the number of lymphocytes expressing forkhead box P3 (Foxp3) was measured by flow cytometry after surface staining with anti-CD4 and anti-CD25. Flow cytometry histograms and graphs of CD4⁺IFN γ ⁺ cells (A, B), CD4⁺IL-4⁺ cells (C, D), CD4⁺IL-17⁺ cells (E, F), and CD4⁺CD25⁺Foxp3⁺ cells (G, H). Note that the administration of MC-MTA significantly reduced the number of CD4⁺ lymphocytes expressing IFN γ , IL-4, or IL-17 and increased the number of CD4⁺CD25⁺Foxp3⁺ lymphocytes compared with the administration of MC-dual target-directed agent (DTA). Values are mean \pm standard error. All results are representative of at least three independent experiments. FITC-A, fluorescein isothiocyanate-A; APC-A, allophycocyanin-A; PE-Cy7-A, phycoerythrin-cyanine-7-A; PE-A, phycoerythrin-A. ^a*p* < 0.05 vs. MC-mock, ^b*p* < 0.05 vs. other groups.

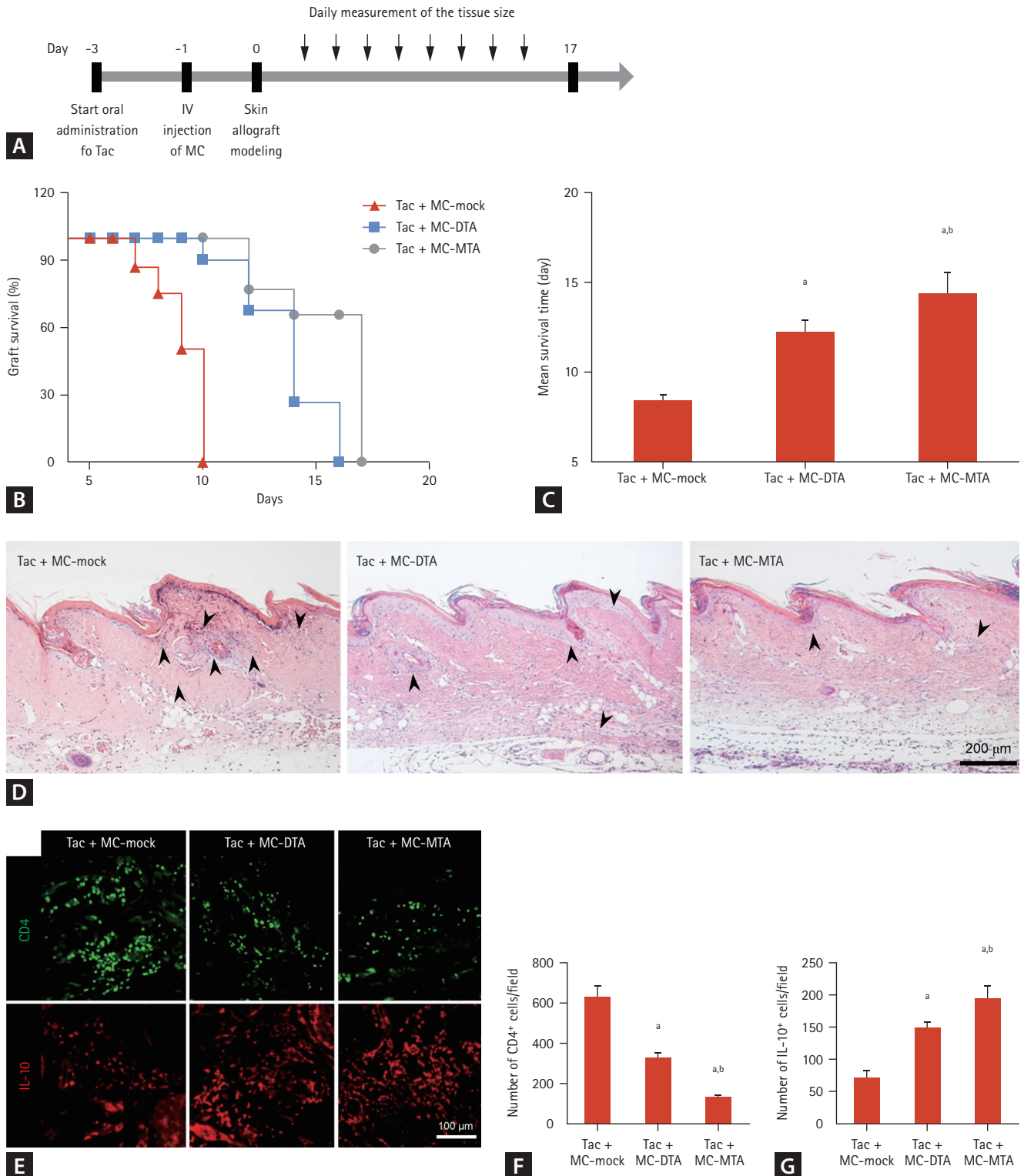


Figure 9. Skin allograft survival in mice treated with Tac and minicircle (MC) encoding multiple target-directed agent (MTA). (A) Diagram of the animal experiment to confirm the effect of the combination of Tac and MC encoding dual target-directed agent (DTA) or MTA in a skin allograft model. (B, C) Survival curve and mean survival times of skin allografts for MC-mock, MC-DTA, or MC-MTA with Tac. (D) Histological changes in skin allografts at day 5 (arrowheads). Hematoxylin and eosin (H&E) staining was performed for each sample. (E, F, G) Representative immunofluorescence image and quantitative analysis for CD4 or interleukin-10 (IL-10) in skin graft at day 5. (E) Scale bar = 200 μm in (D) and 100 μm. Values are mean ± standard error. IV, intravenous. ^a*p* < 0.05 vs. Tac + MC-mock, ^b*p* < 0.05 vs. the other group.

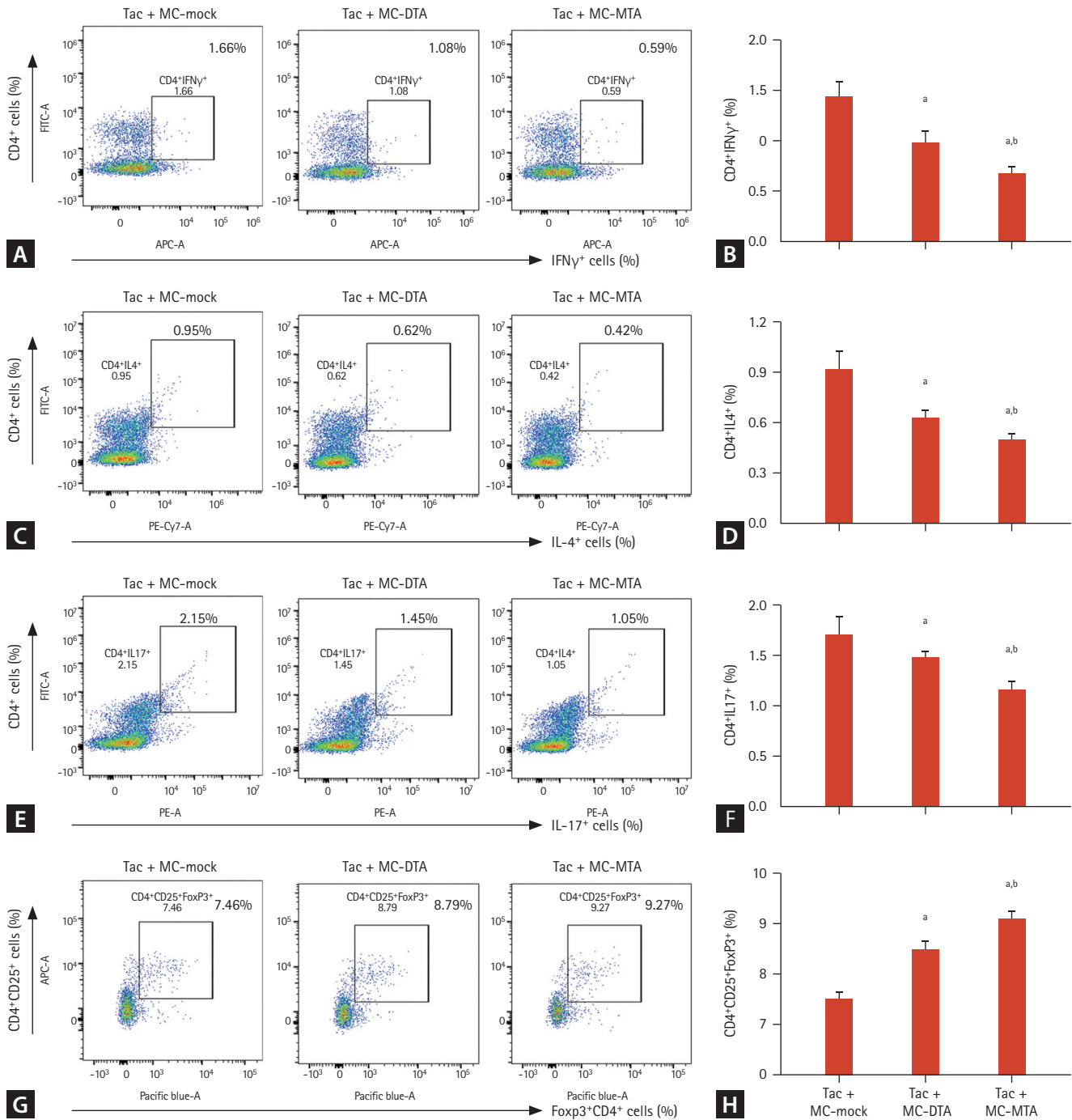


Figure 10. Combined effect of minicircle (MC) encoding multiple target-directed agent (MTA) and Tac on pro-inflammatory T cells and regulatory T cells. Lymphocytes were harvested from the spleens of mice at day 5 after the injection of Tac and MC-dual target-directed agent (DTA) or MC-MTA. Isolated lymphocytes were stimulated for 4 hours *ex vivo* with phorbol myristate acetate and ionomycin in the presence of GolgiStop before being fixed, stained, and permeabilized. After surface staining with anti-CD4, the number of lymphocytes expressing interferon- γ (IFN γ), interleukin-4 (IL-4), or IL-17 was measured by flow cytometry. For the detection of regulatory T cells, the number of lymphocytes expressing forkhead box P3 (Foxp3) was measured by flow cytometry after surface staining with anti-CD4 and anti-CD25. Flow cytometry histograms and graphs of CD4⁺IFN γ ⁺ cells (A, B), CD4⁺IL-4⁺ cells (C, D), CD4⁺IL-17⁺ cells (E, F), and CD4⁺CD25⁺Foxp3⁺ cells (G, H). Note that the administration of Tac + MC-MTA significantly reduced the number of CD4⁺ lymphocytes expressing IFN γ , IL-4, or IL-17 and increased the number of CD4⁺CD25⁺Foxp3⁺ lymphocytes compared with Tac + MC-DTA. Values are mean \pm standard error. All results are representative of at least three independent experiments. FITC-A, fluorescein isothiocyanate-A; APC-A, allophycocyanin-A; PE-Cy7-A, phycoerythrin-cyanine-7-A; PE-A, phycoerythrin-A. ^a*p* < 0.05 vs. Tac + MC-mock, ^b*p* < 0.05 vs. other groups.

Tac + MC-mock, Tac + MC-DTA, or Tac + MC-MTA combination. Starting at 3 days before transplantation, recipient BALB/c mice were administered Tac daily, and MC-mock, MC-DTA, or MC-MTA was injected using the hydrodynamic delivery method 1 day before skin allograft modeling. Several animals were sacrificed for flow cytometry and H&E staining, and the remaining animals were visually inspected daily until complete graft rejection (Fig. 9A). Skin allograft survival in the Tac + MC-DTA group was increased compared with that in the Tac + MC-mock group (MST, 12.3 ± 0.6 days vs. 8.4 ± 0.3 days, $p < 0.05$ vs. Tac + MC-mock). The Tac + MC-MTA group had significantly skin allograft survival compared with the Tac + MC-DTA group (MST, 14.4 ± 1.1 days, $p < 0.05$ vs. Tac + MC-DTA) (Fig. 9B and 9C). Fig. 9E-9G show immunoreactivity for CD4 or IL-10 and the results of the quantitative analysis in the skin allograft tissue section in each group. The number of CD4 positive cells was significantly lower in the Tac + MC-DTA group than in the Tac + MC-mock group ($324 \pm 30/\text{field}$ vs. $629 \pm 56/\text{field}$, $p < 0.05$ vs. Tac + MC-mock group). However, the Tac + MC-MTA group showed a further reduction in the number of CD4 positive cell compared with the Tac + MC-DTA group ($132 \pm 6/\text{field}$, $p < 0.05$ vs. Tac + MC-DTA group). On the contrary, the Tac + MC-MTA group showed a higher number of restored IL-10 cells than the Tac + MC-mock and Tac + MC-DTA groups ($197 \pm 19/\text{field}$ vs. $73 \pm 10/\text{field}$ in the Tac + MC-mock group and $150 \pm 10/\text{field}$ in the Tac + MC-DTA group, $p < 0.05$ vs. Tac + MC-mock and Tac + MC-DTA groups).

Consistent with the graft survival time results, fewer infiltrating cells were detected in the animals injected with Tac + MC-MTA than in those treated with Tac + MC-DTA (Fig. 9D). Flow cytometry also showed that the numbers of CD4⁺IFN γ ⁺, CD4⁺IL4⁺, and CD4⁺IL17⁺ cells were significantly lower in the Tac + MC-MTA group than in the Tac + MC-DTA group (Fig. 10A-10F). The CD4⁺CD25⁺Foxp3⁺ cell population was significantly higher in the Tac + MC-MTA group than in the Tac + MC-DTA group (Fig. 10G and 10H).

DISCUSSION

We have previously suggested a platform system to promote the self-production of therapeutic protein drugs by the host itself [31]. In this study, we evaluated a new synthetic protein drug (anti-CD25 mAb, IL-10, and CXCR3) in

the form of an antibody-cytokine fusion using this system. Injected multiple targeting MCs (MTA) secreted a bioactive form of anti-CD25 mAb, IL-10, and CXCR3 *in vivo*, which was detected in the liver tissue for approximately 40 days. Moreover, mice treated with MCs encoding MTA showed prolonged skin allograft survival time accompanied by improved histologic changes and immunologic regulation. These findings suggest that the MTA protein drug obtained by the MC platform is functionally active and relevant to allograft rejection.

In this study, we used the MC vector for a new protein drug development and verification. Developing protein agents at a small scale is nearly impossible owing to the high cost of their purification and functional characterization. MCs are smaller than conventional plasmids, increasing the probability of cell delivery. Moreover, MCs escape gene silencing and show sustained expression as a result of the unique methylation patterns in these vectors [12]. The present study revealed that *in vivo* MC expression was detected for 40 days and the levels of anti-CD25, IL-10, and CXCR3 showed a 5.9, 3.9, 2.6-fold increase, respectively, in the MC-MTA group compared with the conventional vector (PP-MTA) group. Taken together, the MC system is proposed as a novel platform for the early development of protein drugs.

We selected anti-CD25, IL-10, and CXCR3 as therapeutic targets in an allograft rejection model. Treatments using anti-CD25 antibody agents significantly lower acute rejection rates compared with induction therapy [19,20]. However, the immunosuppressive mechanism of anti-CD25 agents is the deletion of CD25-expressing cells, but it is also has the same effect on Treg cells (FOXP3⁺ and FOXP3⁺CD25⁺ T cells) [21-23], because Treg cells are critical regulators of immune tolerance in transplantation [24,25]. IL-10 conjugation with anti-CD25 antibody compensated for the possibility of Treg downregulation by anti-CD25 during alloimmune response because anti-CD25 targets share the expression of CD25, including both conventional activated T cells and CD4⁺CD25⁺T cells (Tregs) [41,42]. Induction of chemokines during allograft rejection is accompanied by the infiltration of leukocytes bearing the respective chemokine receptors [43]. Of these, CXCR3 is a dominant factor directing T cells into mouse skin allograft confirmed by highly up-regulated T cells in the spleen and allograft from recipients' mouse after transplantation [26]. Based on these findings, we designed MTA structure by the fusion of the anti-CD25 antibody and

the dimer form of IL-10 via short a flexible linker, (G4S1)₃ linker. CXCR3 was connected with IL-10 using (G4S1)₂ linker as shown in Fig. 1.

Next, we examined whether the MTA produced by MCs was produced at sufficient levels to alleviate allograft rejection *in vivo*. We used a highly immunogenic murine skin allograft model and found that the MTA prolonged graft survival compared with MC-mock treatment, accompanied by improved histologic changes and immunologic regulation. We further investigated whether the MTA is effective due to CXCR3, which plays an important role in the migration towards injured or inflamed areas, compared with DTA encoding anti-CD25 and IL-10. First, we performed the *in vitro* transwell migration assay using ligands of CXCL (e.g., CXCL9, 10, 11) and revealed increased migrating cells under CXCL treatment. Second, we tested whether protein drugs were indeed detected around the graft area in the MC-MTA group using MC-MTA vector containing luminescence or RFP fluorescence. Furthermore, the MC-MTA group showed prolonged skin allograft survival, suppression of proinflammatory T cell subset, and induction of regulatory T cells compared with the MC-DTA group, suggesting that CXCR3 may be associated with skin allograft survival.

In clinical practice, combination therapy with a calcineurin inhibitor (CNI) and basiliximab is effective for preventing acute rejection early after KT [20], and is associated with a lower rate of adverse events than the lymphocyte-depleting induction [44]. We found a prolonged skin allograft survival time accompanied by improved histological changes and immunological regulation in the MC-MTA + Tac group compared with the MC-DTA + Tac group. CNI also blocks the T cell receptor-mediated production of IL-2 [45,46] and thus acts synergistically with IL-2 receptor antibodies to limit IL-2-mediated T cell proliferation [47,48]. Moreover, CD25 is upregulated by IL-2 [49,50], and CNI therapy inhibits the activation of marker expression on T cells, including CD25 [50]. Furthermore, enhanced migration function of MTA by CXCR3 may contribute towards promoting the above immunologic benefits. It is therefore conceivable that more intensive immunosuppression and immune tolerance may contribute towards high allograft survival by the combination of MC-MTA and Tac.

The delivery method using the MC system in this study is similar to conventional gene therapy using viral vectors (i.e., plasmid). Previous studies have investigated the delivery of MCs encoding natural inhibitor molecules [13,15,16]. In this

reports, efficient tissue-target gene delivery is important for disease treatment by gene addition correction or knock-down. However, our approach is conceptually different from these approaches. MCs do not require targeting of the vector to the injured tissue or cells (as do current gene therapeutic strategies) because the circulating protein products (MTA) produced by host cells (i.e., liver cells) that take up the MCs treat the disease rather than the manipulation of the host genome in injured cells.

Although the current protocol was effective for the treatment of a mouse skin allograft rejection model, multiple improvements are needed for clinical applications. Clinically acceptable DNA delivery method is required to replace the hydrodynamic injection technique. The jetPEI (Polyplus-transfection SA., Illkirch, France) transfection reagent has already been tested in clinical trials [51], but the drugs' therapeutic levels cannot be obtained while simultaneously avoiding toxicity.

In conclusion, we developed a novel drug comprising anti-CD25/IL-10/CXCR3 using the MC technology system and confirmed its feasibility as a therapeutic tool for preventing allograft rejection in a mouse model. The MC system for synthetic protein drugs is now an emerging concept and may be promising for its cost effectiveness and convenience. We hope that the MC vector system may be useful for the development of novel biological drugs avoiding manufacturing or other practical problems.

KEY MESSAGE

1. We developed a novel drug comprising anti-CD25/interleukin-10 (IL-10)/C-X-C motif chemokine receptor 3 (CXCR3) in the form of an antibody-cytokines fusion using the minicircle technology system.
2. Self-produced anti-CD25/IL-10/CXCR3 by the host were functionally active and reduced allograft rejection in a mouse model.
3. The minicircle vector system may be useful for developing new biological drugs, avoiding manufacturing or practical problems.

Conflict of interest

All authors declare that they have no conflicts of interest with Y-biologics.

Acknowledgments

This work was supported by the Basic Science Research Program through the National Research Foundation of Korea (NRF), funded by the Ministry of Science, Information and Communications Technology (ICT) and Future Planning (NRF-2018R1D1A1A02043014, NRF-2020R1A2C2012711, NRF-2021R1A2C2005192) and the Korean Health Technology R&D Project, Ministry for Health & Welfare, Republic of Korea (HI14C3417).

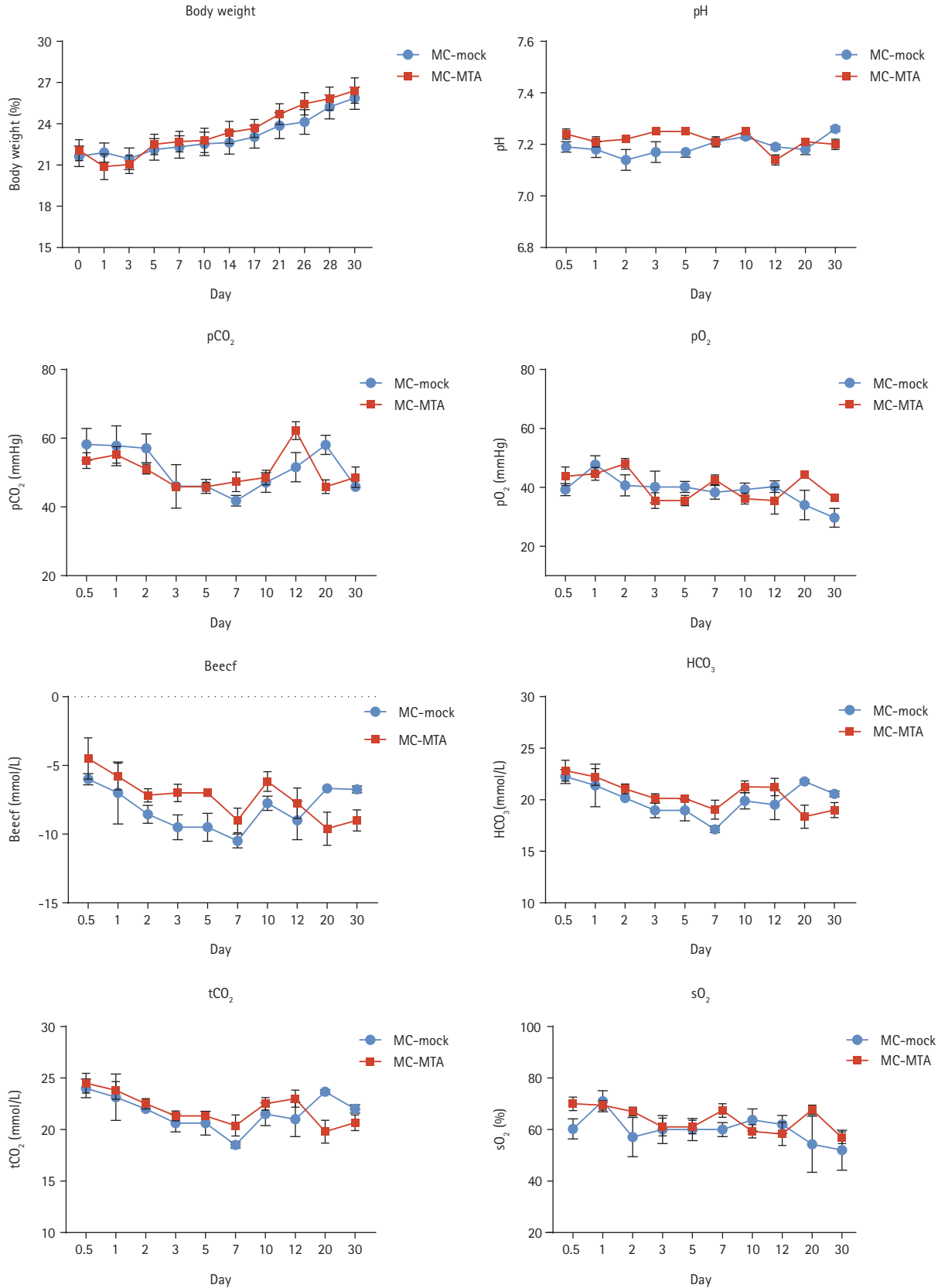
REFERENCES

- Hariharan S, Johnson CP, Bresnahan BA, Taranto SE, McIntosh MJ, Stablein D. Improved graft survival after renal transplantation in the United States, 1988 to 1996. *N Engl J Med* 2000;342:605-612.
- Meier-Kriesche HU, Schold JD, Srinivas TR, Kaplan B. Lack of improvement in renal allograft survival despite a marked decrease in acute rejection rates over the most recent era. *Am J Transplant* 2004;4:378-383.
- Bunnapradist S, Cho YW, Cecka JM, Wilkinson A, Danovitch GM. Kidney allograft and patient survival in type I diabetic recipients of cadaveric kidney alone versus simultaneous pancreas kidney transplants: a multivariate analysis of the UNOS database. *J Am Soc Nephrol* 2003;14:208-213.
- Grenda R. Biologics in renal transplantation. *Pediatr Nephrol* 2015;30:1087-1098.
- Parlakpınar H, Gunata M. Transplantation and immunosuppression: a review of novel transplant-related immunosuppressant drugs. *Immunopharmacol Immunotoxicol* 2021;43:651-665.
- Lu RM, Hwang YC, Liu IJ, et al. Development of therapeutic antibodies for the treatment of diseases. *J Biomed Sci* 2020;27:1.
- Chan AC, Carter PJ. Therapeutic antibodies for autoimmunity and inflammation. *Nat Rev Immunol* 2010;10:301-316.
- McInnes IB, Schett G. Cytokines in the pathogenesis of rheumatoid arthritis. *Nat Rev Immunol* 2007;7:429-442.
- Chen ZY, He CY, Ehrhardt A, Kay MA. Minicircle DNA vectors devoid of bacterial DNA result in persistent and high-level transgene expression in vivo. *Mol Ther* 2003;8:495-500.
- Chen ZY, He CY, Kay MA. Improved production and purification of minicircle DNA vector free of plasmid bacterial sequences and capable of persistent transgene expression in vivo. *Hum Gene Ther* 2005;16:126-131.
- Gill DR, Pringle IA, Hyde SC. Progress and prospects: the design and production of plasmid vectors. *Gene Ther* 2009;16:165-171.
- Gracey Maniar LE, Maniar JM, Chen ZY, Lu J, Fire AZ, Kay MA. Minicircle DNA vectors achieve sustained expression reflected by active chromatin and transcriptional level. *Mol Ther* 2013;21:131-138.
- Zuo Y, Wu J, Xu Z, et al. Minicircle-oriP-IFN γ : a novel targeted gene therapeutic system for EBV positive human nasopharyngeal carcinoma. *PLoS One* 2011;6:e19407.
- Rim YA, Yi H, Kim Y, et al. Self in vivo production of a synthetic biological drug CTLA4Ig using a minicircle vector. *Sci Rep* 2014;4:6935.
- Osborn MJ, McElmurry RT, Lees CJ, et al. Minicircle DNA-based gene therapy coupled with immune modulation permits long-term expression of α -L-iduronidase in mice with mucopolysaccharidosis type I. *Mol Ther* 2011;19:450-460.
- Huang M, Chen Z, Hu S, et al. Novel minicircle vector for gene therapy in murine myocardial infarction. *Circulation* 2009;120(11 Suppl):S230-S237.
- Adamopoulos IE, Tessmer M, Chao CC, et al. IL-23 is critical for induction of arthritis, osteoclast formation, and maintenance of bone mass. *J Immunol* 2011;187:951-959.
- Lim SW, Kim YK, Park N, et al. Application of minicircle technology of self-reproducing synthetic protein drugs in preventing skin allograft rejection. *Ann Transplant* 2015;20:430-440.
- Vincenti F, Kirkman R, Light S, et al. Interleukin-2-receptor blockade with daclizumab to prevent acute rejection in renal transplantation. Daclizumab Triple Therapy Study Group. *N Engl J Med* 1998;338:161-165.
- Nashan B, Moore R, Amlot P, Schmidt AG, Abeywickrama K, Souillou JP. Randomised trial of basiliximab versus placebo for control of acute cellular rejection in renal allograft recipients. CHIB 201 International Study Group. *Lancet* 1997;350:1193-1198.
- Toso C, Merani S, Bigam DL, Shapiro AM, Kneteman NM. Sirolimus-based immunosuppression is associated with increased survival after liver transplantation for hepatocellular carcinoma. *Hepatology* 2010;51:1237-1243.
- Tang Q, Bluestone JA. Regulatory T-cell therapy in transplantation: moving to the clinic. *Cold Spring Harb Perspect Med* 2013;3:a015552.
- Bluestone JA, Liu W, Yabu JM, et al. The effect of costimulatory and interleukin 2 receptor blockade on regulatory T cells in renal transplantation. *Am J Transplant* 2008;8:2086-2096.
- Wood KJ, Sakaguchi S. Regulatory T cells in transplantation

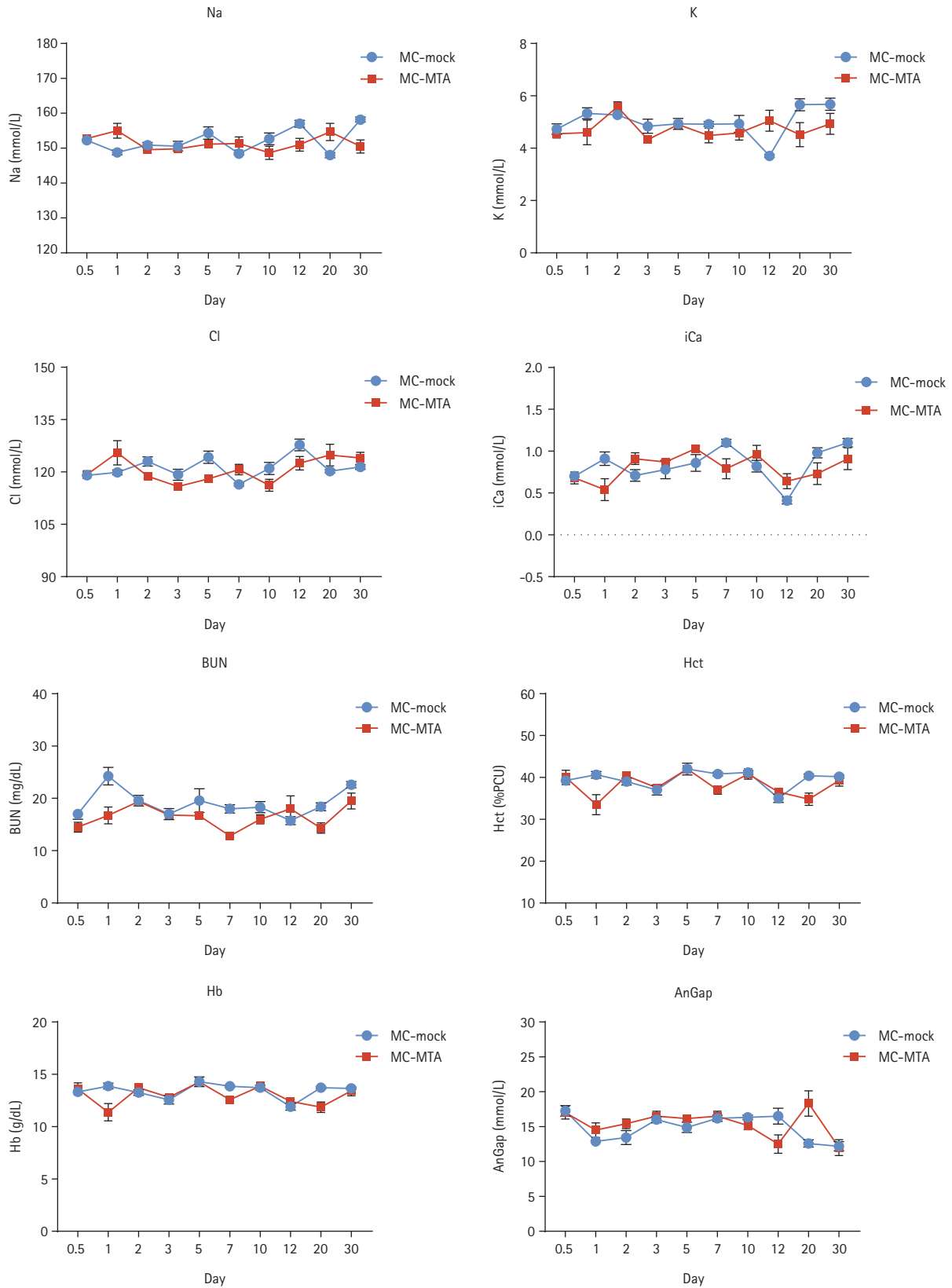
- tolerance. *Nat Rev Immunol* 2003;3:199-210.
25. Sakaguchi S, Sakaguchi N, Shimizu J, et al. Immunologic tolerance maintained by CD25+ CD4+ regulatory T cells: their common role in controlling autoimmunity, tumor immunity, and transplantation tolerance. *Immunol Rev* 2001;182:18-32.
 26. Jiankuo M, Xingbing W, Baojun H, et al. Peptide nucleic acid antisense prolongs skin allograft survival by means of blockade of CXCR3 expression directing T cells into graft. *J Immunol* 2003;170:1556-1565.
 27. Yi H, Kim Y, Kim J, et al. A new strategy to deliver synthetic protein drugs: self-reproducible biologics using minicircles. *Sci Rep* 2014;4:5961.
 28. Kay MA, He CY, Chen ZY. A robust system for production of minicircle DNA vectors. *Nat Biotechnol* 2010;28:1287-1289.
 29. Herweijer H, Wolff JA. Gene therapy progress and prospects: hydrodynamic gene delivery. *Gene Ther* 2007;14:99-107.
 30. McFarland HI, Rosenberg AS. Skin allograft rejection. *Curr Protoc Immunol* 2009;Chapter 4:Unit 4.4.
 31. Lim SW, Shin YJ, Luo K, et al. Host cell in vivo production of the synthetic drug anti-CD25/IL-10 using minicircle vector. *FASEB J* 2019;33:10889-10901.
 32. Maruyama H, Higuchi N, Nishikawa Y, et al. High-level expression of naked DNA delivered to rat liver via tail vein injection. *J Gene Med* 2002;4:333-341.
 33. Wolff JA, Budker V. The mechanism of naked DNA uptake and expression. *Adv Genet* 2005;54:3-20.
 34. Suda T, Liu D. Hydrodynamic gene delivery: its principles and applications. *Mol Ther* 2007;15:2063-2069.
 35. Zhang X, Collins L, Sawyer GJ, Dong X, Qiu Y, Fabre JW. In vivo gene delivery via portal vein and bile duct to individual lobes of the rat liver using a polylysine-based nonviral DNA vector in combination with chloroquine. *Hum Gene Ther* 2001;12:2179-2190.
 36. Andrianaivo F, Lecocq M, Wattiaux-De Coninck S, Wattiaux R, Jadot M. Hydrodynamics-based transfection of the liver: entrance into hepatocytes of DNA that causes expression takes place very early after injection. *J Gene Med* 2004;6:877-883.
 37. Kobayashi N, Nishikawa M, Hirata K, Takakura Y. Hydrodynamics-based procedure involves transient hyperpermeability in the hepatic cellular membrane: implication of a nonspecific process in efficient intracellular gene delivery. *J Gene Med* 2004;6:584-592.
 38. Doh KC, Kim BM, Kim KW, Chung BH, Yang CW. Effects of resveratrol on Th17 cell-related immune responses under tacrolimus-based immunosuppression. *BMC Complement Altern Med* 2019;19:54.
 39. Chung BH, Kim KW, Yu JH, et al. Decrease of immature B cell and interleukin-10 during early-post-transplant period in renal transplant recipients under tacrolimus based immunosuppression. *Transpl Immunol* 2014;30:159-167.
 40. Chung BH, Kim KW, Kim BM, et al. Dysregulation of Th17 cells during the early post-transplant period in patients under calcineurin inhibitor based immunosuppression. *PLoS One* 2012;7:e42011.
 41. Sadlack B, Merz H, Schorle H, Schimpl A, Feller AC, Horak I. Ulcerative colitis-like disease in mice with a disrupted interleukin-2 gene. *Cell* 1993;75:253-261.
 42. Malek TR. T helper cells, IL-2 and the generation of cytotoxic T-cell responses. *Trends Immunol* 2002;23:465-467.
 43. Nelson PJ, Krensky AM. Chemokines, chemokine receptors, and allograft rejection. *Immunity* 2001;14:377-386.
 44. Lebranchu Y, Bridoux F, Buchler M, et al. Immunoprophylaxis with basiliximab compared with antithymocyte globulin in renal transplant patients receiving MMF-containing triple therapy. *Am J Transplant* 2002;2:48-56.
 45. Heidt S, Roelen DL, Eijsink C, et al. Calcineurin inhibitors affect B cell antibody responses indirectly by interfering with T cell help. *Clin Exp Immunol* 2010;159:199-207.
 46. Hamawy MM. Molecular actions of calcineurin inhibitors. *Drug News Perspect* 2003;16:277-282.
 47. Ueda H, Cheung YC, Masetti P, et al. Synergy between cyclosporine and anti-IL-2 receptor monoclonal antibodies in rats: functional studies of heart and kidney allografts. *Transplantation* 1991;52:437-442.
 48. Ueda H, Hancock WW, Cheung YC, Diamantstein T, Tilney NL, Kupiec-Weglinski JW. The mechanism of synergistic interaction between anti-interleukin 2 receptor monoclonal antibody and cyclosporine therapy in rat recipients of organ allografts. *Transplantation* 1990;50:545-550.
 49. Reem GH, Cook LA, Palladino MA. Regulation of interleukin-2 synthesis in human thymocytes. *J Biol Response Mod* 1984;3:195-205.
 50. Welte K, Andreeff M, Platzer E, et al. Interleukin 2 regulates the expression of Tac antigen on peripheral blood T lymphocytes. *J Exp Med* 1984;160:1390-1403.
 51. Buscail L, Bournet B, Vernejoul F, et al. First-in-man phase 1 clinical trial of gene therapy for advanced pancreatic cancer: safety, biodistribution, and preliminary clinical findings. *Mol Ther* 2015;23:779-789.

SUPPLEMENTARY METHODS

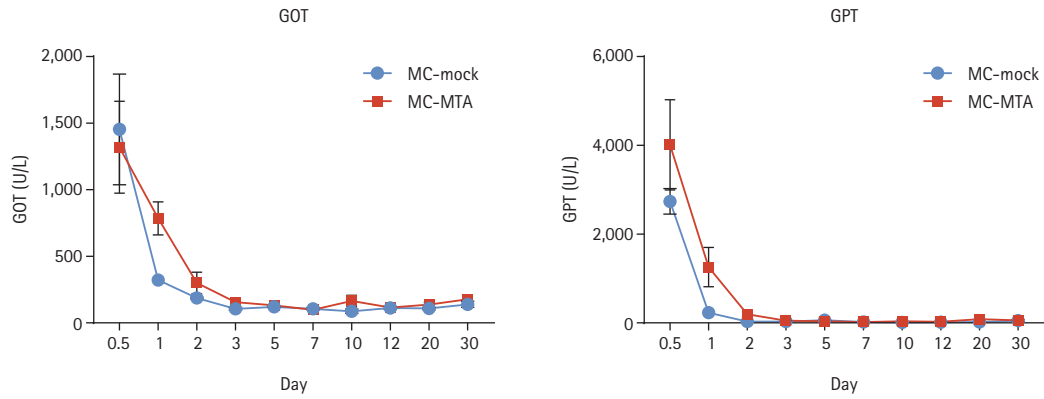
All procedures were performed in strict accordance with the recommendations of the ethical guidelines for animal studies. All experimental animal care protocols were approved by the Animal Care and Use Committee of the Catholic University of Korea (CUMC-2018-0130). Minicircle (MC)-mock or MC-multiple target-directed agent (MTA) were delivered 1 day before measuring body weight and basic functions using the hydrodynamic tail-vein injection. Animals in each group measured body weight and collected blood at indicated day. Basic functions of animals in each group were analyzed using portable Abbott i-STAT analyzer (Abbott Point of Care, East Windsor, NJ, USA) using G3+ cartridge for blood gases and Chem8+ cartridge for chemistries/electrolytes in whole blood. Assay for glutamate oxaloacetate transaminase and glutamate pyruvate transaminase in serum was run at the equipment Fuji Dri-Chem NX500 (Fujifilm Corp., Tokyo, Japan) according to the manufacture's recommendations.



Supplementary Figure 1. Body weight and basic functions using G3+ cartridge. MC, minicircle; MTA, multiple target-directed agent.



Supplementary Figure 2. Basic functions using Chem8+ cartridge. MC, minicircle; MTA, multiple target-directed agent; BUN, blood urea nitrogen; Hct, hematocrit; Hb, hemoglobin; AnGap, anion gap.



Supplementary Figure 3. Liver function. GOT, glutamate oxaloacetate transaminase; GPT, glutamate pyruvate transaminase; MC, mini-circle; MTA, multiple target-directed agent.

Supplementary Table 1. Nucleotide sequences of protein drugs

Nucleotide	Nucleotide sequences
Anti-CD25HC/IL-10/ CXCR3	CATGGCAACCATGGGTTGGAGTTACATAATACTGTTTTTGGTGGCGACCGCAGCGGACGTCCATTCCCAATTG- CAACAGTCCGGCACAGTTCTGGCCAGGCCTGGAGCCAGTGTGAAAATGTCCTGTAAAGCCAGCGGTTACT- CATTACACGATACTGGATGCACTGGATTAAGCAACGGCCCGGTCAAGGCTTGGAGTGGATCGGGGC- GATTTACCCCGGTAACCTCAGACACGTCATATAACCAAAAAGTTTGAAGGTAAGGCTAAGCTGACTGCTGTCA- CATCAGCAAGTACTGCATATATGGAGCTGAGTAGTTTGACCCACGAAGACTCAGCAGTATACTACTGCTC- CCGAGATTATGGCTACTATTTTACTTCTGGGGTCAGGGGACGACGCTCACGGTTAGCTCTGCAAGTAC- CAAAGGTCCAAGTGTCTTCTCTCGCCCCCTCCAGTAAGAGTACTAGTGGCGGAAGTGCAGGCTCTCGGTTG- CCTCGTAAAGGACTACTTCCCGGAACCGGTCACGGTCTCATGGAACCTGCGGGCGTTGACCTCCGGCGTTCA- CACCTTCCGGCCGACTGCAATCTAGTGGACTTACTCTCTCAGTAGTGTGTCACGGTTCCCTCCAGCTCCCT- GGGCACACAGACTTATATATGCAACGTAAACCATAAGCCATCAAATACTAAGGTCGATAAAAAGAGTGGAG- CCCCCAAAAGTTGCGATAAGACTCACACTTGCCCGCCATGCCAGCGCCTGAGCTTTTGGGAGGTCCAT- CAGTTTTTCTGTTTCCGCCAAAACCGAAGGACACACTGATGATCAGCCGGACTCCTGAGGTTACATGTGTGTC- GTTGATGTGTCTCACGAAGATCCCGAAGTAAAGTTCAATTGGTATGTAGATGGCGTAGAGGTACATAATGCTA- AAATAAACCGCGGGGAAGAGCAATATAATTCCACATACAGAGTAGTTTCTGTGCTGACAGTACTTTCATCAG- GATTGGCTTAACGGCAAGGAGTATAAATGTAAAGTTTCAAATAAAGCGTTGCCGCGCCATCGAGAAGAC- GATCAGCAAAGCGAAAGGACAGCCGAGAGAACCTCAAGTGTACTCTCCCTCCTTCTCGGGACGAGCT- TACTAAAAACCAAGTCAGCCTCACCTGCCGTTAAAGGGTTTCTATCCTTCTGATATAGCAGTAGAGTGGGAAT- CAAATGGACAACAGAGAATAACTATAAGACCACCCCTCCAGTACTTGATTCAGACGGTTCCCTTTTTCTG- TATAGCAAACCTTACTGTAGACAAGAGTAGGTGGCAACAAGGGAACTGTTCTCTTGTCTAGTATGATGAAAG- CACTTACATAACCTATACTCAAAGAGCCTTCTACTGAGCCAGTAAGGGAGGGGGAGGTAGCGGCGGAG- GAGGGAGTGGGGGCGGGGGCTCTAGCAGGGGGCAATATCCAGGGAAAGATAATAATGTACTCATTTCCTCGT- AGGCAATCCCATATGCTGCTGGAGCTTCAACCGCTTGTAGTCAAGGATTTCTTTTCAAACAAAAGAC- CAGTTGGACAACATTTTGTACCGACAGTCTTATGCAAGATTTCAAGGGATATCTTGGATGCCAAGCACT- TAGTGAGATGATACAGTTTTACTTGGTTGAGGTAATGCCACAAGCTGAGAAGCACGGCCAGAAATCAAG- GAGCACCTCAACAGCTTGGGGGAAAAACTTAAACACTGCGGATGCGACTGCGGAGGTGCCATCGCTTCCCTC- CCTGCGAAAACAAGTCTAAAGCCGTTGAGCAGGTGAAATCCGACTTAAATAAGCTCCAGGACCAGGGAG- TATACAAGGCAATGAATGAATTCGACATCTTTATAAACTGCATTGAAGCATATATGATGATCAAGATGAAAAGT- GGAGGAGGAGGGTCTGGCGGAGGAGGGTCAATGGTTCTCGAAGTCTTGACCATCAGGTCCTAATGATGCA- GAGGTGCGAGCCCTTTGGAGAAGTTTCTAGCTCTTATGATTATGGTGAAAATGAGTCAGATTCTTGTGCA- CAAGCCACCTTGCCCCAAGATTTACAGCTTGAACCTCGACAGGGGATCC
Anti-CD25LC	GCTAGCATGGCCACCATGGGATGGAGCTATATCCTCTTTTTGGTGGCCACAGCGGCCGATGTCCACTCG- CAGATTGTGTCTACACAGAGCCCCGCCATCATGAGCGCCTCTCCAGGCGAGAAAGTGACCATGACATGTAGCG- CCAGCAGCAGCAGATCTACATGCAGTGGTATCAGCAGAAGCCCGGCACAAGCCCCAAGAGATGGATCTAC- GATACCAGCAAGCTGGCCTCTGGCGTGCCAGCCAGATTTTCTGGCTCTGGCAGCGGCACCAGCTACAGCCT- GACAATCTCTAGCATGGAAGCCGAGGACGCCGCCACCTACTACTGTACCAGAGAAGCAGCTACACCTTCG- GCGGAGGCACCAAGCTGGAAATCAAGAGAACAGTGGCCGCTCCGAGCGTGTTCATCTTTCCACCAAGCGAC- GAGCAGCTGAAGTCTGGCACAGCCTGTGCTGTGCTGCTGAACAACCTTACCCTCGGGAAGCCAAGGTG- CAGTGAAGGTGGACAATGCCCTGCAGAGCGGCAATAGCCAAGAGAGCGTGACCGAGCAGGACAGCAAG- GACTCTACCTACTCTGAGCAGCACCTGACACTGAGCAAGGCCGACTACGAGAAGCACAAGGTGTACG- CCTGTGAAGTGACACACCAGGGCCTGAGCAGCCCTGTGACCAAGAGCTTCAATAGAGGCGAGGGATCC

HC, heavy chain; IL-10, interleukin-10; CXCR3, C-X-C motif chemokine receptor 3; LC, light chain.

Supplementary Table 2. Peptide sequences of protein drugs

Protein	Peptide sequences
Anti-CD25HC/IL-10/ CXCR3	MATMGWSYIILFLVATAADVHSQLQQSGTVLARPGASVKMMSCKASGYSFTRYWMHWIKQRPQGQLEWIGAIYPGNS-DTSYNQKFEGKAKLTAVTSASTAYMELSSLTHEDSAVYYCSRDYGYFDFWGGQTTTLVSSASTKGPSVFPLAPSSKSTS-GGTAALGCLVKDYFPEPVTVSWNSGALTSVHTFPAVLQSSGLYSLSSVVTVPSSSLGTQTYICNVNHHKPSNTKVD-KRVEPPKSCDKTHTCPPCPAPPELLGGPSVFLFPPKPKDTLMISRTPEVTCVVVDVSHEDPEVKFNWYVDGVEVHNAK-TKPREEQYNSTYRVVSVLTVLHQDWLNGKEYKCKVSNKALPAPIEKTISKAKGQPREPQVYTLPPSRDELTKNQVSLT-CLVKGFPYPSDIAVEWESNGQPENNYKTTPPVLDSDGSFFLYSKLTVDKSRWQQGNVFCFSVMHEALHNHYTQKSLSL-SPGKGGGGSGGGGSSRGQYSREDNCTHFPVGGQSHMLLELRRTAFSQVKTFQTKDQLDNILLTDSLMDQ-FKGYLGCQALSEMIQFYLVVMPQAEKHGPEIKEHLNSLGEKLTLMRLRRCHRFLPCENKSKAVEQVKSDFNKLQD-QGVYKAMNEFDIFINCIEAYMMIKMKSGGGGGSGGGGSMVLEVSDHQVLNDAEVAALLENFSSSYDYGENESD-SCCTSPPCPQDFSLNFDGRS
Anti-CD25LC	MATMGWSYIILFLVATAADVHSQIVSTQSPAIMASASPGEKVTMTCSASSRSYMQWYQKPGTSPKRWIYDTSK-LASGVPARFSGSGSGTSYSLTSSMEAEADAATYYCHQRSSYTFGGGKLEIKRTVAAPSVFIFPPSDEQLKSGTASVCLLN-NFYPREAKVQWKVDNALQSGNSQESVTEQDSKSTYLSSTLTLSKADYEKHKVYACEVTHQGLSSPVTKSFNRGEGS

HC, heavy chain; IL-10, interleukin-10; CXCR3, C-X-C motif chemokine receptor 3; LC, light chain.

Supplementary Table 3. Peptide sequences of protein drugs

Protein	Peptide sequences
Anti-CD25HC	ATMGWSYIILFLVATAADVHSQLQQSGTVLARPGASVKMSCKASGYSFTRYWMHWIKQRPQGLEWIGAIYPGNSDT- SYNQKFEKGAKLTAVTSASTAYMELSSLTHEDSA VYYCSRDYGYDFWGGTTLTVSSASTKGPSVFLAPSSKSTSGG- TAALGCLVKDYFPEPVTVSWNSGALTSGVHTFPAVLQSSGLYSLSSVTVPSSSLGTQTYICNVNHHKPSNTKVDRVEP- PKSCDKTHTCPPCPAPELLGGPSVFLFPPKPKDTLMISRTPEVTCVVVDVSHEDPEVKFNWYVDGVEVHNAKTKPRE- EQYNSTYRVVSVLTVLHQDWLNGKEYKCKVSNKALPAPIEKTISKAKGQPREPQVYTLPPSRDELTKNQVSLTCLVKG- FYPSDIAVEWESNGQPENNYKTTTPVLDSDGSSFFLYSKLTVDKSRWQQGNVFCFSVMHEALHNHYTQKSLSLSPGK
Anti-CD25LC	ATMGWSYIILFLVATAADVHSQIVSTQSPA IMSASPGKVTMTCSASSRSYMQWYQQKPGTSPKRWIYDTSK- LASGVPARFSGSGSGTSYSLTISMEAEADAATYYCHQRSSYTFGGGKLEIKRTVAAPS VFIFPPSDEQLKSGTASVCLLN- NFYPREAKVQWKVDNALQSGNSQESVTEQDSKDYSLSTLTKADYEKHKVYACEVTHQGLSPVTKSFNRGE
IL-10-anti-CD25HC	ATMGWSYIILFLVATAADVHSSPGQGTQSENSCTHFPGNLPNMLRDLRDAFSRVKTFQMKDQLDNLNLLKESLLEDFK- GYLGCQALSEMIQFYLEEVMQAENQDPDIKAHVNSLGENLKTLRLRRLRCHRFLPCENKSKAVEQVKNAFNKLQEK- GIYKAMSEFDIFINYIEAYMTMKIRNGGGGGGGGGGGSSQLQQSGTVLARPGASVKMSCKASGYSFTRYWM- HWIKQRPQGQLEWIGAIYPGNSDTSYNQKFEKGAKLTAVTSASTAYMELSSLTHEDSA VYYCSRDYGYDFWGGQ- GTTTLTVSSASTKGPSVFLAPSSKSTSGGTAALGCLVKDYFPEPVTVSWNSGALTSGVHTFPAVLQSSGLYSLSSVTV- VPSSSLGTQTYICNVNHHKPSNTKVDRVEPPKSCDKTHTCPPCPAPELLGGPSVFLFPPKPKDTLMISRTPEVTCVVVD- VSHEDPEVKFNWYVDGVEVHNAKTKPREEQYNSTYRVVSVLTVLHQDWLNGKEYKCKVSNKALPAPIEKTISKAKGQ- PREPQVYTLPPSRDELTKNQVSLTCLVKG FYPSDIAVEWESNGQPENNYKTTTPVLDSDGSSFFLYSKLTVDKSRWQQGN- VFSCFSVMHEALHNHYTQKSLSLSPGK
IL-10	ATMGWSYIILFLVATAADVHSSPGQGTQSENSCTHFPGNLPNMLRDLRDAFSRVKTFQMKDQLDNLNLLKESLLEDFK- GYLGCQALSEMIQFYLEEVMQAENQDPDIKAHVNSLGENLKTLRLRRLRCHRFLPCENKSKAVEQVKNAFNKLQEKGI- YKAMSEFDIFINYIEAYMTMKIRN

HC, heavy chain; LC, light chain; IL-10, interleukin-10.